THE 2 TO 7 MICRON INFRARED ABSORPTION SPECTRA OF THE WATER ADSORBED ON LITHIUM-, SODIUM-, POTASSIUM-, AND CALCIUM-BENTONITE

by

Garrison Sposito

A Thesis Submitted to the Faculty of the

DEPARTMENT OF AGRICULTURAL CHEMISTRY AND SOILS

In Partial Fulfillment of the Requirements

For the Degree of

MASTER OF SCIENCE

In the Graduate College

UNIVERSITY OF ARIZONA

1963

STATEMENT BY AUTHOR

This thesis has been submitted in partial fulfillment of requirements for an advanced degree at the University of Arizona and is deposited in the University Library to be made available to borrowers under rules of the Library.

Brief quotations from this thesis are allowable without special permission, provided that accurate acknowledgment of source is made. Requests for permission for extended quotation from or reproduction of this manuscript in whole or in part may be granted by the head of the major department or the Dean of the Graduate College when in their judgment the proposed use of the material is in the interests of scholarship. In all other instances, however, permission must be obtained from the author.

SIGNED: Garrison Sposito

APPROVAL BY THESIS DIRECTOR

This thesis has been approved on the date shown below:

DUWAYNE M. ANDERSON
Professor of Agricultural Chemistry and Soils

April 29 - 1963
Date

ACKNOWLEDGMENT

The writer wishes to express his deepest gratitude to Dr. Duwayne M. Anderson, without whose guidance, trust, and implicit belief in the scientific method this thesis, in its present form, would not have been possible.

To Dr. Raymond J. Hannapel, for his uncommon acumen and many helpful suggestions which intensified the intellectual atmosphere about the writer throughout his graduate studies, and to Dr. Wallace H. Fuller, for his liberal administration which permitted the writer to obtain without restriction the educational background required for the undertaking of the thesis research, to these men, also, gratitude is expressed.

Lastly, but in a certain sense most importantly, the writer wishes to acknowledge the patience and understanding of his wife, Volney, who so many times through sheer determination alone has transformed what seemed to be failure into achievement, what seemed to be success into perspective.

TABLE OF CONTENTS

TABLE OF CONTENTS (Continued)

LIST OF TABLES

LIST OF ILLUSTRATIONS

INTRODUCTION

Although many studies of the behavior of montmorillonite-water systems have been made, none of them as yet has provided the necessary basis for the development of a statistical thermodynamic theory of adsorbed water: the methods of nearest-neighbor lattice statistics, which show promise for giving a second-order description of the adsorbed state, permit the specification of the equilibrium thermodynamic behavior of a substance only after the nature of its configuration and potential energy states is known. In response to this lack of information, this thesis contains the results of what is believed to be a novel approach to quantitatively describing the adsorbed water lattice. The 2 to 7 micron infrared absorption spectra of the water adsorbed by Li-, Na-, K-, and Ca-bentonite have been recorded with the purpose of introducing the absorption frequencies near 3 microns into a semi-empirical theory of the hydrogen bond. This treatment of the data has yielded an estimate of the dimensions and dissociation energies of the hydrogen bonds of the adsorbed water lattice and, hopefully, has provided a part of the experimental nucleus of a future thermodynamic theory of adsorbed water. The molecular data, in addition, have been

discussed with respect to the dimensions of the idealized structures that have been proposed for adsorbed water and with respect to the mean hydrogen bond dissociation energies calculated from the heats of desorption of water on the four bentonite salts that were investigated.

LITERATURE REVIEW

That the water in the interlayer region and along the crystal fractures of montmorillonite is different from ordinary water in bulk is generally accepted as fact. However, considerable debate continues over what is the exact geometric configuration and potential energy distribution among the adsorbed water molecules. In this section the geometric and thermodynamic properties of the water adsorbed by montmorillonite will be reviewed and then used to evaluate the proposals that have been made for the structure of water on clay surfaces. On the basis of this evaluation a new hypothesis concerning the nature of the interlayer water will be developed and an experimental means will be suggested for testing it in part.

The Geometric Properties of Water Adsorbed on Montmorillonite

The properties of the first stable interlayer hydrate, i.e., when moisture content is independent of the relative humidity, on montmorillonite[1] appear to depend upon both the mineral surface and its exchange-

---

[1] Throughout this discussion the structure of montmorillonite will be assumed to be essentially the same as that of pyrophyllite. A confirmation of this supposition can be found (cont'd on next page)

able cations. X-ray diffraction data taken under varying humidity conditions at 20° C. by Cornet (13), Mering (39), and Mooney et al. (41) showed that Na-montmorillonite forms a single-layer hydrate at a relative vapor pressure near 0.3. By contrast, Ca-montmorillonite was observed by these investigators to form a two-layer hydrate at this relative pressure. The diffraction data obtained at 30° C. by Hendricks et al. (23) using the same clay salts indicated that the relative pressure at which the stable hydrate forms shifts upward with increasing temperature, more so with Na-clay than with Ca-clay. These results exemplify the greater role played by the exchangeable calcium ion, since it possesses a greater ability to hydrate than sodium ion, in forming the water structure on montmorillonite.

The extent of the interaction an exchangeable cation has with the adsorbed water layer, as well as the structural ramifications of that interaction, can be estimated from a knowledge of the hydration number of the cation when it is bound into the first stable interlayer hydrate. Hendricks et al. (23) calculated the hydration numbers of the exchangeable cations on Li-, Na-, K-, and Ca-montmorillonites of known moisture content using the differential thermal analysis (DTA) curve of each.

---

[1] (Cont'd from p. 3) in a recent article by D. M. C. MacEwan called "Montmorillonite Minerals" in The X-ray Identification and Crystal Structures of Clay Minerals. G. Brown, ed. Mineralogical Society, London, 1961.

By assuming the weight of water bound to the cations to be proportional to the area under the high-temperature (240° C.) portion of the first endothermic peaks, the number of water molecules per exchangeable cation could be computed. In this way, the hydration number of calcium ion on montmorillonite was found to be six, that of lithium, three, and that of sodium and potassium, zero. The conclusion regarding the sodium and potassium ions was reached because no high temperature endothermic peaks were observed for the Na- and K-clays.

Mooney et al. (41) have made a similar calculation from their desorption isotherms for several homoionic Wyoming bentonites.[2] Assuming the large exchangeable cations on Rb- and Cs-montmorillonite were unhydrated, they attributed all the water determined to be on these clays at monolayer coverage to mineral surface hydration only. The mean weight of this water was subtracted from the monolayer water contents of the Ca- and Li-clays in order to calculate the hydration numbers of the exchangeable ions. Calcium was found to have a hydration number of eight while that of lithium was apparently just one. Because no theoretical monolayer water content could be ascertained for the Na- and K-clays, no hydration numbers were estimated for the exchangeable cations on them. However, it should be pointed out that these calculations of the hydration number, based upon a theoretical monolayer water content

---

[2] The term "bentonite" is a generic name for any montmorillonite formed in situ from argillaceous tuff.

and the assumed nonhydration of exchangeable Rb and Cs, imply unwarrented conclusions about the nature of the hydration state of the exchangeable cations in the stable adsorbed water configuration. This is especially true in the case of Ca-clay since the "monolayer" water content calculated by Mooney et al. is shown by their own x-ray diffraction data to correspond in reality to a double layer of water molecules between the internal surfaces of Ca-clay. Thus, the calculated hydration number of eight for exchangeable calcium need not be doubled to indicate the coordination of this cation with the water molecules in the first stable hydrate. Moreover, it seems unreasonable to assume that the Rb- and Cs-clays have entirely unhydrated exchangeable cations. Perhaps a more appropriate method of calculating the hydration of the mineral surface than that of Mooney et al. is to subtract the estimated water of hydration of Rb and Cs from the monolayer water contents of their respective clay salts. If this is done, assuming the aqueous solution hydration number of 1.2 for both exchangeable ions (21), and the resulting mean water content for mineral surface hydration used to obtain new coordination numbers for the exchangeable Ca and Li ions (considering the former ion to be in a two-layer hydrate at the theoretical "monolayer" water content), hydration numbers of about 5 and 3, respectively, are found. These values are essentially the same as those determined by Hendricks et al. (23) and, as will be shown later,

are the most compatible with other structural data for adsorbed water on Ca- and Li-montmorillonites.

Besides the above-mentioned criticisms, it should be stated that an unjustifiable conclusion would be reached if it were assumed that no stable interlayer hydrate existed for the Na- and K-clays studied by Mooney et al. simply because water vapor adsorption by these clays did not conform to theory and allow a monolayer water content to be calculated. A similar statement can be made for the DTA data and conclusions of Hendricks et al. (23) for Na- and K-montmorillonite.

A detailed consideration of the hydration numbers given above is worthwhile at this point as it can possibly shed some light on the geometric arrangement of the interlayer water molecules in montmorillonite. Calcium ion, for example, appears to be in octahedral coordination with the nearest adsorbed water molecules surrounding it. Therefore, one would expect the water on Ca-clay to be oriented either in a continuous, two-dimensional network of octahedra or in scattered, locally-ordered octahedral groups about the exchangeable cations with disordered, or at least differently oriented, water filling in on the rest of the mineral surface. Since surface heterogenieties are predominant on montmorillonite, owing to the variability of its interlayer charges resulting from random isomorphous substitution in the tetrahedral and octahedral layers of the mineral, and since the adsorptive force about the calcium

ion is of comparatively short range, the second type of water structure suggested seems the more probable.

Although the lithium ion appears to have a low hydration number at the monolayer moisture content, its radius-ratio with the water molecule predicts octahedral coordination of the cation. The calculation made by Hendricks et al. was for Li-montmorillonite in an atmosphere of only five per cent relative humidity, which seems too low for the formation of a stable hydrate since even Ca-clay could not form one until placed in an atmosphere of 40 per cent relative humidity. At a relative vapor pressure near 0.40, the data of Hendricks showed that Li-clay appeared to have two water layers associated with it, one which could be removed entirely at low temperature (160° C.) and one which could not. It is possible that these layers, when near an exchange site, are coordinated about the lithium ion in planar groups of three water molecules per layer. Because of the small size and charge of the cation, the second and most distant layer of water molecules could be bound with less force than the first layer and, therefore, be removed at a lower temperature. The two-layer water structure thus formed on Li-clay would be similar in appearance to that on Ca-clay, but should be less stable, both thermally and mechanically, owing to the smaller affinity the lithium ion has for the second layer of water (21, 41). For the same reason, when the first monolayer forms on Li-clay it may be nearly as stable as the two-layer hydrate.

It is not reasonable to believe, as the data of Mooney et al. (41) and Hendricks et al. (23) seem to indicate, that the exchangeable cations on Na- and K-clays are completely without effect on the water structures in the interlayers of these minerals. The lack of any high temperature endothermic peaks for the water on a clay salt may indicate either that the hydration water is bound as strongly to the cation as to the mineral surface or that the cation, for steric reasons, tends to have the same water structure about it as would the clay surface in the absence of the cation. Because both sodium and potassium are only slightly hydrated in solution (hydration numbers of 3.5 and 1.9, respectively, 21) and because both are small enough in size to be occluded in a "fixed" state by montmorillonite (this phenomenon will be discussed more fully later), it is possible that both structural mechanisms mentioned above are operative on Na- and K-clays.

The properties of water in thick bentonite suspensions, while applicable to the water at low coverage on montmorillonite only in a qualitative sense, are still of interest since they provide evidence for an increased ordering of structure in the adsorbed phase as compared to the free liquid phase of water. Low (32), for example, has determined the ionic mobilities of the chloride salts of lithium, sodium, and potassium ions in bentonite pastes and found them to be always lower than the corresponding ones for the salts in pure solution. The decrease in ionic mobility he interpreted as mainly the result of not only a

different but more ordered structure in adsorbed water than in free water. In the converse of the aforementioned experiment, Low (33) determined the temperature dependence of the rate of flow of water through initially-saturated Na-bentonite. The temperature coefficient, i.e., the apparent activation energy, ranged from 3.9 to 4.4 kcal. per mole, depending upon and increasing with the time the saturated clay stood before the initiation of flow. Noting that the apparent activation energy for the viscous flow of ordinary water in the same temperature range as his experiments was 3.9 kcal. per mole, Low concluded as before that the increase in apparent activation energy was due to a time-dependent, clay-induced water structure which was more crystalline than that of ordinary water.

Additional evidence for the concept of an ordered water structure comes from the experiments of Anderson and Low (3). These investigators determined the densities of water adsorbed by Li-, Na-, and K-bentonites in suspension from accurate plots of clay-water volume against moisture content. The slope of the curve gave the partial specific volume of the adsorbed water, the reciprocal of which is its density. This method suffers from none of the uncertainties of interpretation of the more conventional pycnometer method of determining densities. At a calculated distance of about 10 A. from the clay surface, the density of adsorbed water was 0.975, 0.972, and 0.981 gm. per $cm.^3$

at 25° C. on the Li-, Na-, and K-clay, respectively. These values, all about two percent lower than the 0.997 gm. per $cm.^3$ observed for pure water at 25° C., show conclusively the combined effects of the clay surface and its exchangeable cations on the adsorbed water structure: a configuration of water molecules somewhat more oriented than is liquid water must exist to at least three monomolecular layers away from the clay surface.

The Energy State of Water Adsorbed on Montmorillonite

Calorimetric heat of immersion data for homoionic montmorillonites have repeatedly shown that the decreasing order of heats of immersion is Ca-clay > Na-clay > K-clay (44, 53). Since this series is in the same order as the heats of solution of the exchangeable cations (5), one may infer that the adsorbed ion plays an important role in determining the energy state of the water on montmorillonite. Zettlemoyer et al. (61) concur with this conclusion on the basis of their heat of immersion measurements with degassed, natural Wyoming bentonite (essentially a Na-montmorillonite). Although the adsorption isotherms at 25° C. for the clays evacuated at 100° C. and 25° C. displayed no difference in shape, indicating no structural difference in the mineral surface presented to the adsorbate, the heats of immersion of the two degassed media at 25° C. were 21.0 and 12.9 cal. per gm. clay, respectively. The

difference between heats of immersion was concluded to be the result of the greater heat of solution of the exchangeable ions dehydrated at 100°C.; however, clay lattice defects must also be important adsorption sites on a bare clay surface.

The differential heats of desorption[3] for water on the Wyoming bentonite previously evacuated at 100° C. were calculated by Zettlemoyer from heat of immersion and adsorption isotherm data taken at 25° C. For a relative vapor pressure of zero, the q_{diff} value was 36.0 kcal. per mole of water; at a relative pressure of 0.3, that required for monolayer formation, q_{diff} had dropped to 17.5 kcal. per mole. These data, however, are questionable because Zettlemoyer used an adsorption isotherm rather than a desorption isotherm to transform the heat of immersion--initial relative vapor pressure plot to a heat of immersion--initial water content plot to calculate q_{diff}. Since desorption isotherms are always displaced more toward the water content axis than adsorption isotherms, it is likely that the heat of desorption values given above are too high. An approximate recalculation, using the desorption isotherm for Wyoming bentonite determined by Mooney et al. (40) instead of

---

[3] The differential heat of desorption is defined by

$$q_{diff} = E_v - (\delta Q/\delta m)_T \qquad [1]$$

where q_{diff} is the differential heat of desorption, E_v is the heat of vaporization of liquid water, and $(\delta Q/\delta m)_T$ is the slope of a heat of immersion--initial water content plot.

Zettlemoyer's data, results in q_{diff} values of 17.6 kcal. per mole and 12.4 kcal. per mole at 0.0 and 0.3 relative vapor pressure, respectively. These figures are more reasonable than Zettlemoyer's as they are comparable with all other heat of desorption values reported for Wyoming bentonite and similar clays.

Another important indicator of the clay surface-adsorbed water binding energy is the isosteric heat of desorption, defined by the equation[4]

$$q_{iso} = R\, T_2 T_1 / T_2 - T_1 \ln P_2 / P_1 ,$$

an integrated form of the Clausius-Clapeyron equation, where T is the absolute temperature, P is the water vapor pressure, and R is the ideal gas constant. The isosteric heat of desorption, calculated from desorption isotherms made at two proximate temperatures, is based upon the assumption of ideal gas behavior for the adsorbate vapor and, therefore, gives only an approximation of the differential heat of desorption. Takizawa (54) has found the isosteric heat of desorption for the water adsorbed by a Japanese bentonite to be 27.0 kcal. per mole of water when the moisture content of the clay was 0.01 gm. water per gm. clay; 18.5 kcal. per mole when 0.05 gm. water per gm. clay were present, and

---

[4] This definition of q_{iso} is that given by S. Brunauer in The Adsorption of Gases and Vapors. I. Physical Adsorption. Princeton University Press, Princeton, New Jersey, 1945, p. 225.

11.5 kcal. per mole when the moisture content reached 0.100 gm. water per gm. clay. Monolayer adsorption was calculated to occur at a water content of about 0.06 gm. water per gm. clay. The differences between Takizawa's values and those recalculated from Zettlemoyer's data at very low moisture content probably reflect to some extent the heterogeneity to be found among the adsorption sites on the clays they studied. The degree of hydration and charge of the exchangeable cation, the presence of broken bonds originating in the tetrahedral and octahedral layers, as well as the amount of water-adsorbing impurities, such as free silica and the iron- and aluminum-hydroxy compounds, all serve to contribute to the observed heat of interaction between water vapor and clay. Considering the broad range of relative importance possible for each of these factors among montmorillonites, it would be hardly more than fortuitous if the calculated values of the heats of interaction at low moisture content were exactly the same for different clays, even if their pretreatment were the same.

Mooney et al. (40) calculated q_{iso} from desorption isotherms they obtained at 0 and 20° C. for Na-bentonite[5] initially degassed at 70° C. They found values ranging from 13.3 kcal. per mole at a moisture content of 0.039 gm. water per gm. clay to 11.5 kcal. per mole at 0.150 gm.

---

[5] These data are, perhaps, only approximate since the bentonite, prepared from a H-Al (electrodialyzed) clay, was probably a Na-Al-clay rather than a pure Na-clay.

water per gm. clay; monolayer formation was estimated to occur at 0.122 gm. water per gm. clay.

An indirect estimate of the differential heat of desorption is found in the constant "C" of the Brunauer-Emmett-Teller theory of multilayer adsorption (8). If it is assumed that the differential heat of desorption of all water layers but the first is equal to the heat of vaporization of pure water, then the differential heat of desorption at the water content corresponding to monolayer coverage is given by

$$E_1 = RT \ln \left(Ca_2 / a_1\right)\left(b_1 / b_2\right) + E_v \qquad [2]$$

where C is the BET constant, a and b are constants, and E_v, R, and T have their previous significance. The ratio a_2b_1 / a_1b_2 is usually considered to be unity.

Orchiston (43) has found the values of E_1 (actually, an approximate E_1 since adsorption isotherms, which are not reproducible, were used in obtaining it) for a degassed Arizona montmorillonite to be in the same order as observed in heat of immersion data: Ca-clay, 12.4 kcal. per mole; Na-clay, 11.5 kcal. per mole; and K-clay, 11.3 kcal. per mole. The BET plots of Mooney et al. (41) indicate E_1 values of 12.4 kcal. per mole and 12.8 kcal. per mole for water on Ca-bentonite and Li-bentonite, respectively. It must be remembered, however, that the Ca-clays at BET "monolayer" coverage actually have two water layers associated with them instead of one so that E_1 here applies to a double-layer hydrate.

Takizawa (54) has found the temperature dependence of E_1 for a Japanese bentonite to be about three times as great as that of the heat of vaporization of liquid water in the temperature range 15-35° C. Such behavior may indicate that the adsorbed molecules have considerable ability to move two dimensionally on the clay surface since the temperature dependence of the heat of desorption (and vaporization) is directly related to the heat capacity at constant pressure and thus to the internal degrees of freedom of the adsorbed molecules.

The fact that E_1, q_{iso}, and q_{diff} recalculated from Zettlemoyer's data are each slightly greater at the monolayer water content than the heat of vaporization of pure water (10.5 kcal. per mole at 25° C.) suggests, as did the structural data in the previous section, that the completed adsorbed water structure is a little more ordered than that of liquid water. The general validity of this statement can be demonstrated further through a calculation of the entropy change which water molecules undergo in the transition from the liquid phase to the configuration of the first stable interlayer hydrate on Li-, Na-, and Ca-montmorillonite. Assuming that the Ca and Li ions were each in a double-layer hydrate and that the Na and K ions were in single-layer structures, approximate entropies of desorption were computed from the definition of the Gibbs free energy and the sorption isotherms and E_1 values of Mooney et al. (41) and Orchiston (43); the entropy changes for water

undergoing the liquid-adsorbed phase transition were then calculated by subtracting the entropy of vaporization from the entropy of desorption and changing the sign of the result. The following values were obtained: Li-clay, -2.6 cal. per mole per °C. (20° C.); Na-clay, -0.9 e.u. per mole (25° C.); K-clay, -0.6 e.u. per mole (25° C.); and Ca-clay, -2.6 e.u. per mole (20° C.). These results may be compared with the entropy change for the water (25° C.) -ice (0° C.) transition, which is -5.4 e.u. per mole. That the entropy state of water on the Na- and K-clays is not markedly different from that of liquid water, while that of the water on the Li- and Ca-clays is somewhat more akin to that of ice is in accordance with the structural and thermodynamic data that have been presented and, as will be shown later, is further evidence in favor of the conclusions to be drawn from infrared spectra regarding the structures of adsorbed water on these minerals.

Proposals for the Structure of Water Adsorbed on Montmorillonite

As may have been inferred from the discussion in the previous pages, little experimental evidence exists pertaining to the exact configuration of the water molecules adsorbed by montmorillonite. The best descriptions of crystal structure so far have been provided from x-ray diffraction data since the relative intensities of the planar reflections can be transformed through Fourier synthesis into a distribution

function giving the location of the atoms in a unit cell of the crystal lattice. However, since clays, especially montmorillonite, are seldom obtained as single crystals, but more often as slightly oriented flakes in the powder form, a complete Fourier analysis based upon the diffraction pattern of the interlayer region has been impossible to perform. For these reasons proposals for the geometric configuration of adsorbed water on montmorillonite and other layer silicates have been relegated to speculation based upon tenuous experimental data, except for the outstanding work of Mathieson and Walker (38) to be discussed later.

Upon discovering that the water on montmorillonite gave basal reflections corresponding to a water layer about 3 A. thick on the mineral surface, Hendricks and Jefferson in 1938 (22) were the first to propose a definite structure for adsorbed water. They suggested that the water molecules were cast into hexagonal groups as a net extending over the basal surfaces. The stability of the structure was to come from the intermolecular hydrogen bonds forming the hexagonal groups and from the fact that the oxygen atoms of the basal planes to which the water molecules were bound were themselves disposed into a hexagonal net. The water structure thus was viewed as an extension of the clay mineral surface. Assuming the a and b dimensions of the water net were identical to those of montmorillonite, the separation of water molecules in the planar hexagonal groups would be 3.0 A. The coplanar

groups themselves were assumed to lie parallel with the montmorillonite surface at a distance of 2.73 A.

Although this proposal explained the observed x-ray diffraction pattern of hydrated montmorillonite, it has been justifiably criticized because it did not account for the presence of exchangeable cations (36, 59). Moreover, the adsorbed water molecules forming the coplanar hexagonal groups would have to undergo an increase in the HOH bond angle of about 16° over the 104° 31' observed for the water vapor molecule (24); this change is three times that of the water molecule undergoing the vapor-ice transition (47). Such a distortion should, at best, make the Hendricks-Jefferson structure highly unstable, if not impossible. Therefore, considering also the influence of mineral surface heterogeneities, it would seem that the Hendricks-Jefferson proposal could be feasible only if it were to exist in an especially irregular, metastable state characterized by relatively weak intermolecular bonding and if it were to suffer very little disruptive effect from the exchangeable cations on the mineral surface.

Barshad (4) has considered the structure of adsorbed water in the light of his theoretical calculations of the basal spacings one would expect for various types of water adsorption. He postulated that the monolayers are discontinuous at low moisture contents with the molecules tending to form tetrahedra with the oxygen atoms of the clay mineral surface. As the water content increased, the adsorbed water would

form more closely-packed layers consisting of hexagonal rings as proposed by Hendricks and Jefferson. Contrary to other opinion, the exchangeable cations were expected by Barshad to modify but not seriously alter the formation of the water structure.

Low (34) has suggested two mechanisms of clay-water interaction which could result in a modified Hendricks-Jefferson water net. He noted that although covalent hydrogen bonding between the basal surface and the water molecules is likely, since isomorphic substitution permits the lone pair electrons of the surface oxygen atoms to be easily distorted, at low water contents hydration of the exchangeable cations should result in the polarization of the surrounding water molecules with the consequent disruption of the adsorbed water lattice, and London dispersion forces might occur between the mineral surface and the bound water to produce a compressed double layer for short distances. Because the clay surface is irregular and the interactions suggested above could take place concurrently, Low concluded reasonably that the structure of adsorbed water is not hexagonal ice, as proposed by Macey (35).

Forslind (16) postulated that the adsorbed water molecules on montmorillonite bond covalently with the calcium and lithium ions. In the case of the former, the bonds would be octahedrally coordinated and resonate between two ionic and one neutral state of the cation. The lithium ion, having a lower electronegativity than the calcium ion,

would form but one covalent bond rotating among various positions in the Li-H_2O structure. The result of these two bonding situations would be a controlling influence on the structural arrangement of the surrounding adsorbed water lattice. The monovalent cations with lower electronegativities than lithium, such as sodium and potassium, would be expected to exert only a small disturbing effect on the surrounding water.

The relatively strong H_2O-divalent cation interaction is also emphasized in the structure which Mathieson and Walker (37, 38, 58) have devised for the adsorbed water on Mg-vermiculite based upon x-ray diffraction studies of that mineral. The surface structures of vermiculite and montmorillonite are similar enough to warrant the extension of their proposal to water adsorbed by the latter. Electron density maps constructed by these investigators from a complete Fourier analysis of a single crystal of hydrated vermiculite showed that the water molecules did not fluctuate randomly about their calculated mean positions on the clay surface, but were regularly displaced from them in one direction. Mathieson and Walker concluded from these results that the network of water molecules covering the fully-hydrated vermiculite is partially distorted, containing two layers of molecules disposed in groups of six around each possible cationic site. This would allow approximately one site in three to have an undistorted hydration hull, corresponding well with the number of such sites required by the

observed exchange capacity of vermiculite. The magnesium ions were thought to be able to diffuse freely through the interstices of nearby hydration hulls, which were thought to be in a state of constant reordering, as well as through unfilled cationic sites. The hydrated phase of the Mg-vermiculite studied by Mathieson and Walker had a basal spacing of 14.36 A. with bond lengths in the interlayer region as follows: H_2O-H_2O within a water layer near a cationic site, 2.97 A.; H_2O-H_2O between layers, 2.78 A.; H_2O-O, 2.90 A; and Mg-H_2O, 2.11 A. These values were regarded as precise to within 0.04 A.

Walker (57) has also shown that the postulated water structure suffers changes throughout dehydration, becoming increasingly distorted as the clay hydrate is heated. A second stable hydrate having a basal spacing of 13.82 A. is formed when the magnesium ions begin to draw the weakly-bound water molecules from nearby unfilled cationic sites. The removal of a small amount of water from the 13.82 A. phase results in an abrupt contraction of the basal spacing to 11.59 A. Here, there is but one layer of water molecules interleaved between the silicate layers so that the magnesium ions are now forced to occupy imperfect octahedral environments consisting of three water molecules and three silicate oxygen atoms. This behavior tends to support the view expressed previously that the adsorbed water structure is thermally metastable.

Rowland et al. (50) have made diffraction patterns for several homoionic Wyoming bentonites and a vermiculite while heating them

from 25° C. to 900° C. After comparing the bentonite patterns with that for vermiculite, they suggested, in accordance with the conclusions drawn earlier from the discussion of the hydration states of these clays, that Ca- and Li-montmorillonite have octahedrally-coordinated exchangeable cations and that these cations are bound into a water lattice having the Mathieson-Walker structure. For the Na- and K-clays, as might be expected since the exchangeable cations on these minerals are unlike magnesium, only single-layer hydrates were found.

The general impression that one may derive from examining the data concerning the properties of adsorbed water on montmorillonite and comparing these data to the proposals just enumerated is that any comprehensive description of the water lattice in terms of its configuration and energy states must necessarily be complex. No generalization as to structure can be made which does not account for the mutual interaction of the mineral surface with the exchangeable cations; the adsorption of water by the nonargillaceous compounds present in clays, such as the iron and aluminum hydroxides and the amorphous silica precipitates; the structural heterogeneity of the clay surface; the presence of broken bonds and polymeric metal precipitates at the edges of the clay crystals, and the existence of adsorbed air and organic compounds on the mineral surface. No generalization as to energy state is possible without noting the extent of hydrogen and Van der Waal's bonding probable with regard to the affinity for water of both the exchangeable cations

and the clay mineral; the effect of temperature on the formation of a stable water lattice; the energies required for the diffusion of water molecules and the exchangeable cations along the clay surface, and the existence of a spectrum of energies for the adsorption sites on both the clay and the compounds commonly found associated with it. The labyrinthine factors participating in the formation of a stable water configuration demand the complex view. One is forced to consider a water lattice characterized by regions of local order: local order around the exchangeable cations, around the corners and edges of the clay crystal, around the precipitated compounds coating the mineral surface; local order around every possible adsorption site, depending entirely upon the energy state of the site, its geometry, and the relative advantage it has for coming into contact with and orienting free water molecules entering the adsorptive force fields of the clay crystal. While it is true that often one kind of adsorption site takes precedence on a given clay mineral, the influence of increasing temperature upon the stability of the water lattice is probably great enough to seriously alter the intersite equilibrium among the adsorbed molecules to the extent of changing the predominant structural arrangement and adsorption site several times before dehydration is complete. In the last analysis one must regard the structure of adsorbed water as a constantly changing flux of intermolecular attractions and repulsions

characterized by complex equilibrium micro-states intelligibly relatable only by their relative probability for existing under a given set of environmental conditions.

Infrared Studies of the Water Adsorbed on Montmorillonite

As stated in the preceding discussion, the complexity of the arrangement of the water lattice on montmorillonite cannot be treated in a comprehensive manner unless every factor contributing to its existence is correctly accounted for. In the author's opinion this cannot be done without including both the configuration and the energy state of adsorbed water in the experiments used to probe the interlamellar region. For this reason the methods of infrared spectroscopy should increase in use and value as the procedures for applying them to clay-water systems are developed: the wavelength at which infrared radiation is absorbed by a compound is directly related to its energy state, while the frequency at which the compound absorbs can be related through the quantum-statistical theory of molecular vibrations to its equilibrium bond lengths. Thus, a method exists in principle for finding the configuration and energy state of a molecule from a single experiment. Because hydrogen bonding is likely to be a principal factor in water lattice formation and because the semirandom order of clay powder samples should have no effect on the wavelength at which

the water lattice absorbs in the infrared (even if it were crystalline) since ice has been shown not to possess dichroism under ordinary conditions (42), an infrared study of adsorbed water on montmorillonite should prove to be a valuable means of estimating the geometric configuration of water molecules wherever they are hydrogen-bonded on the clay surface.

The infrared spectra taken of water on montmorillonite have generally been for the purpose of qualitative rather than quantitative structural analysis. One of the first investigations was reported by Buswell, Krebs, and Rodebush in 1937 (10), who studied the 3 micron infrared spectrum of a natural Wyoming bentonite and found absorption bands centered at 3631[6] and 3410 $cm.^{-1}$ which they assigned to the unbonded hydroxyls and adsorbed water, respectively. They also noted that the variation in intensity of the former band with time of drying at 100° C. was far less than that of the latter. Later, Buswell and Dudenbostel (9) obtained the spectra of homoionic Wyoming bentonite films dried on microscope slide covers. Bands at 3630 and 3400 $cm.^{-1}$ were observed, irrespective of the exchangeable cations on the clays. However, the order of decreasing absorbance was Ca-clay > Li-clay > K-clay > Na-clay, possibly indicating the order of water contents in the

---

[6] Band centers in absorption spectra will be given in $cm.^{-1}$. The relation between this unit and that of wavelength is $\omega = 10^4/\lambda$ where λ is in microns and ω is in $cm.^{-1}$.

clay salts. Adler and co-workers (1) have confirmed the existence of bands around 3630 and 3400 cm.$^{-1}$ for Wyoming bentonite from their work on the reference clay minerals. It should be pointed out that certain of their data are not acceptable as spectra of adsorbed water since some of the samples were pretreated with propyl alcohol.

Roy and Roy (51) have questioned the assignment of the absorption band at 3400 cm^{-1} as the vibrational mode of hydrogen-bonded adsorbed water. They found that several clays dried at 250° C. and pressed in KBr produced absorptions near 3400 cm.$^{-1}$. Since it seemed unlikely to them that water could persist in the clays at high temperatures, they concluded that the 3400 cm.$^{-1}$ band could not always be attributed to adsorbed water. The results are not conclusive for two reasons. First, the dried clays were not pressed into the KBr under dessicant conditions and, therefore, may have picked up some atmospheric water. The very rapid adsorption of water vapor by clean surfaces is well known: Mooney et al. (40), for example, observed that their degassed clays took up 90 per cent of the equilibrium water content a few minutes after exposure to water vapor. Secondly, Roy and Roy also reported an absorption band near 1600 cm.$^{-1}$ for their dried clays. This frequency, that normally associated with the bending vibration of the water molecule, indicates by its presence that adsorbed water may yet have been on the clays.

Spectra recently taken of highly dessicated montmorillonites and other similar layer silicates (6, 15, 27, 52) appear to show that the band at 3630 $cm.^{-1}$ refers to the vibration frequency of the clay lattice hydroxyls. However, since adsorbed water can persist in these minerals until 400° C. (18), the assignment cannot be made unequivocally.

Fripiat et al. (18) have obtained spectra of homoionic Camp-Berteau montmorillonite films. The absorption of the adsorbed water in the 3 and 6 micron regions was studied as a function of temperature in the range 20 to 400° C. Plots of the relative absorbance of the water at 3 microns against temperature showed that even at 400° C. some water remained in the clays, irrespective of the exchangeable cations on them. Because x-ray diffraction patterns showed that the interlayers of the clays collapsed near 150° C., Fripiat and co-workers were led to postulate that the residual water molecules must lie either in the hexagonal cavities of the internal surface or on the external surface. The former hypothesis was favored. To prove it, the temperature dependence of the absorption intensity at 3 microns for Na-kaolinite was compared to that for Na-montmorillonite. At 90° C. the intensities of the bands for kaolinite had dropped 85 per cent, while those for the montmorillonite bands had fallen only 20 per cent. Because kaolinite has no internal surfaces, the difference in dehydration behavior was taken as evidence that the residual water molecules on montmorillonite

lie in the interlayer region. This conclusion, however, rests on the tacit assumption that the bonding of water with the kaolinite surfaces is equal in strength to its bonding with the montmorillonite external surfaces. Because the former mineral has hydroxylic surfaces, one would expect the hydrogen bonding of water to kaolinite to be less covalent than to montmorillonite, as suggested by Low (34). For this reason it would also be weaker.

A second proof of their hypothesis is cited by Fripiat and coworkers. They found 10.9 per cent moisture in a potassium-montmorillonite film dried at 105° C., near the temperature of interlayer collapse for this clay salt. Allowing 5 per cent for clay lattice water, they calculated 5.9 per cent or 3.3 mmoles hydration water per gm. clay to be present at this temperature. If the water molecules were spread on an external surface of 80 $m.^2$ per gm., they speculated, hexagonal packing would require three monomolecular layers to be present. Since this is very unlikely at 105° C., the residual water must be in the interlayers. The questionable assumption here is that the external surface of K-montmorillonite is but ten per cent of the total surface. Bower and Gschwend (7) find the surface area of K-bentonite, as measured by ethylene glycol retention, is reduced only 35 per cent when the clay salt is heated from room temperature to 600° C. Using the 725 $m.^2$ per gm. clay Fripiat et al. found with ethylene glycol as the total specific surface of Camp-Berteau montmorillonite, an external surface of about

470 $m.^2$ per gm. clay is implied. From electron micrographs and the unit cell dimensions of montmorillonite an external surface of 345 $m.^2$ per gm. clay can be calculated. Either figure reduces the three monolayers computed by Fripiat to be on heated K-montmorillonite to a more reasonable one-half monolayer. Unless this and the previously cited difficulty can be overcome, it does not seem possible to accept the hypothesis that the residual water in montmorillonite is necessarily to be found in the interlayer region.

The strength of the hydrogen bond in water is usually considered an approximately linear function of the difference between the unbonded and hydrogen-bonded stretching frequencies of the hydroxyls (48, p. 83). Fripiat et al. have found the frequency difference for adsorbed water on montmorillonite to be somewhat dependent upon the exchangeable cation present. The frequency shifts were in the order Sr-clay > Na-clay > K-clay > Li-clay at 25° C., while at 250° C. they were in the order K-clay > Na-clay > Li-clay > Sr-clay.

It can be seen from the foregoing discussion that the possibilities for studying the properties of adsorbed water by infrared methods are in an early stage of development. Up to the present time, a high resolution infrared absorption spectrum in the 3 and 6 micron regions has not been reported for adsorbed water. Such data, if accurate, could be introduced into the appropriate quantum-statistical equations to give an

estimate of the lengths of the intermolecular hydrogen bonds in the adsorbed water lattice, together with the dissociation energies of these bonds. In the pages to follow, the results of an attempt at obtaining accurate infrared absorption spectra in the 2-7 micron region for four homoinic montmorillonites and treating these data theoretically are reported.

THEORY

This section consists of two parts: the derivation and simple application of the time-independent Schrödinger wave equation in one dimension and a quantum-mechanical, empirical theory of the hydrogen bond. In presenting the foundations of wave mechanics, an intuitive rather than mathematically rigorous approach has been used which owes its development largely to the textbooks of Pauling and Wilson (46), Rojansky (49), and Callen (11). The theory of the hydrogen bond given here is due to Lippincott and Schroeder (29, 30), although the presentation is slightly different in form from that in their publications so that continuity may be preserved. An elementary knowledge of second-order differential equations, infrared absorption, and the mechanics of molecular vibrations has been assumed and is necessary for comprehending the theory to follow. For the unfamiliar, Herzberg (24) provides an excellent introductory review of these topics.

The Schrödinger Wave Equation

Derivation and relation to classical mechanics

The behavior of a particle moving in a conservative, one-dimensional force field (Cartesian coordinate frames) is specified by the Lagrangian function, L,

$$L = T(\dot{x}) - V(x) \qquad [1]$$

where T is the kinetic energy of the particle, and V is its potential energy. The function T is itself defined by

$$T = 1/2\ m\dot{x} \qquad [2]$$

where m is the particle mass, and $\dot{x}$ is the first time derivative of the position coordinate, or, the speed. Thus

$$L = 1/2\ m\dot{x} - V(x) \qquad [3]$$

It is desirable to make a partial Legendre transform of the Lagrangian so as to obtain a function of the momentum and position of the particle, rather than its speed and position. This transform produces a new function called the Hamiltonian, H, defined by

$$-H = L(P,x) - Px \qquad [4]$$

where P is the partial Legendre transform of the Lagrangian with respect to the velocity, and L and x have their previous significance. The function P is defined as

$$P = \delta L / \delta \dot{x} = p_x \qquad [5]$$

and is called the momentum of the particle. By performing the operation shown in equation [5] and inserting the result into equation [4], the relation

$$H = p_x^2/2m + V(x) \qquad [6]$$

is derived. The significance of the Hamiltonian may be seen by taking its first derivative with respect to time, using equation [4]:

$$\frac{dH}{dt} = P\ddot{x} + \dot{P}\dot{x} - (\delta L/\delta x)\,\dot{x} - (\delta L/\delta P)\,\dot{P} = 0 \qquad [7]$$

since $\delta L/\delta x = \dot{P}$ and $\frac{\delta L \delta P}{\delta P \delta t} = \frac{\delta L}{\delta x}\,\frac{\delta^2 x}{\delta t \delta P}\,\frac{\delta P}{\delta t} = P\ddot{x}$. The Hamiltonian is therefore a constant of the motion and is called the total energy of a particle in a conservative force field.

The particle described classically by equation [6] can be treated as a wave when two assumptions[7] are made. They are as follows:

1. The physical properties of any dynamical variable pertaining to a given dynamical system can be inferred theoretically from the mathematical properties of an operator to be associated with this dynamical variable.

2. The operators α and β, to be associated, respectively, with the dynamical variables α and β, must be chosen so that

---

[7] For a discussion of these assumptions, see Rojansky, V. Introductory Quantum Mechanics. Prentice-Hall, New York, 1938, pp. 72-75.

$$\alpha\beta - \beta\alpha = i\hbar [\alpha, \beta] \qquad [8]$$

where $i^2 = -1$, $\hbar$ is Planck's constant divided by 2π, and $[\alpha, \beta]$ is the operator to be associated with the classically-computed Poisson bracket of α and β. (This latter quantity is just the expanded Jacobian $\delta(\alpha, \beta) / \delta(\alpha, \beta)$.)

With the momentum and position as the dynamical variables, equation [8] becomes

$$xp_x - p_x x = i\hbar \qquad [9]$$

since $[x, p_x]$ is classically unity. The choice of the operators to be associated with x and p_x is facilitated by examining the identity obtained from differentiating a product and multiplying through by $i\hbar$:

$$x (- i\hbar \, d/dx) - (- i\hbar \, d/dx) \, x = i\hbar. \qquad [10]$$

Evidently, the linear operator to be associated with x is just x itself, while that to be associated with p_x is $- i\hbar \, d/dx$. Consequently, the operator associated with the Hamiltonian must be

$$H = -\hbar^2/2m \; d^2/dx^2 + V(x) \qquad [11]$$

when the results of equation [10] are substituted into equation [6]. The equation [11] is useful when calculating the quantum-mechanical energy states of a particle if the "proper value" of the linear operator H can be found. Such "proper values" are termed "eigenvalues," and must satisfy the relation

$$H\psi = E\psi \qquad [12]$$

where H is the linear operator associated with the variable ψ, and E is the "eigenvalue" of H. Therefore the total energy, E, of the particle can have only certain "eigenvalues" characteristic of the operator H. This is equivalent to saying that the particle receives energy in a discrete rather than continuous manner.

When equation [11] is introduced into equation [12], the relation

$$-\hbar^2/2m \; d^2\psi/dx^2 + V(x)\psi = E\,\psi \qquad [13]$$

is derived. This equation can be rearranged to have the more familiar form

$$d^2\psi/dx^2 + 8\pi^2 m/h^2 \,(E - V(X)\,\psi = 0 \qquad [14]$$

which is the time-independent Schrödinger wave equation in one dimension.

Solutions of the wave equation for the one-dimensional, finite potential energy well

The function ψ in equation [14] is defined as the "eigenfunction" of the linear operator H so long as it is well-behaved. This means that ψ (x) and $d\psi/dx$ must be continuous for all x; that $\psi(x)$ is finite when $x \rightarrow \pm\infty$; and that $\psi(x)$ is not identically zero. The physical significance of ψ is that it is the de Broglie wave amplitude for a particle with momentum p_x such that

$$\lambda = h/p_x \qquad [15]$$

where λ is the de Broglie wavelength and h is Planck's constant. The function $|\psi|^2$ (since ψ may be complex) is proportional to the probability of finding a particle of momentum p_x in space. The solutions of equation [14], therefore, are used to find the most probable position of some particle when its energy state is known, or vice versa.

Figure 1 is a diagram of a rectangular potential energy well. Such a well is a good approximation of the potential energy state of a molecular harmonic oscillator whose line spectrum is discrete rather than continuous. The appropriate form of equation [14] for this problem is

$$\psi'' + k(E - V(x)) = 0 \qquad [16]$$

where the prime, for convenience, refers to the derivative with respect to x, and k is $8\pi^2 m/h^2$. The values of V(x) for the various regions are

$$\begin{aligned} V &= 0 && x < -x_1 \\ V &= -e^2/x_o && -x_1 < x < x_1 \\ V &= 0 && x > x_1 \end{aligned} \qquad [17]$$

The second of equations [17] is the coulombic potential for a particle with charge e. Because V(x) is discontinuous, well-behaved solutions of equation [16] are different for each region of figure 1. The appropriate differential equations are

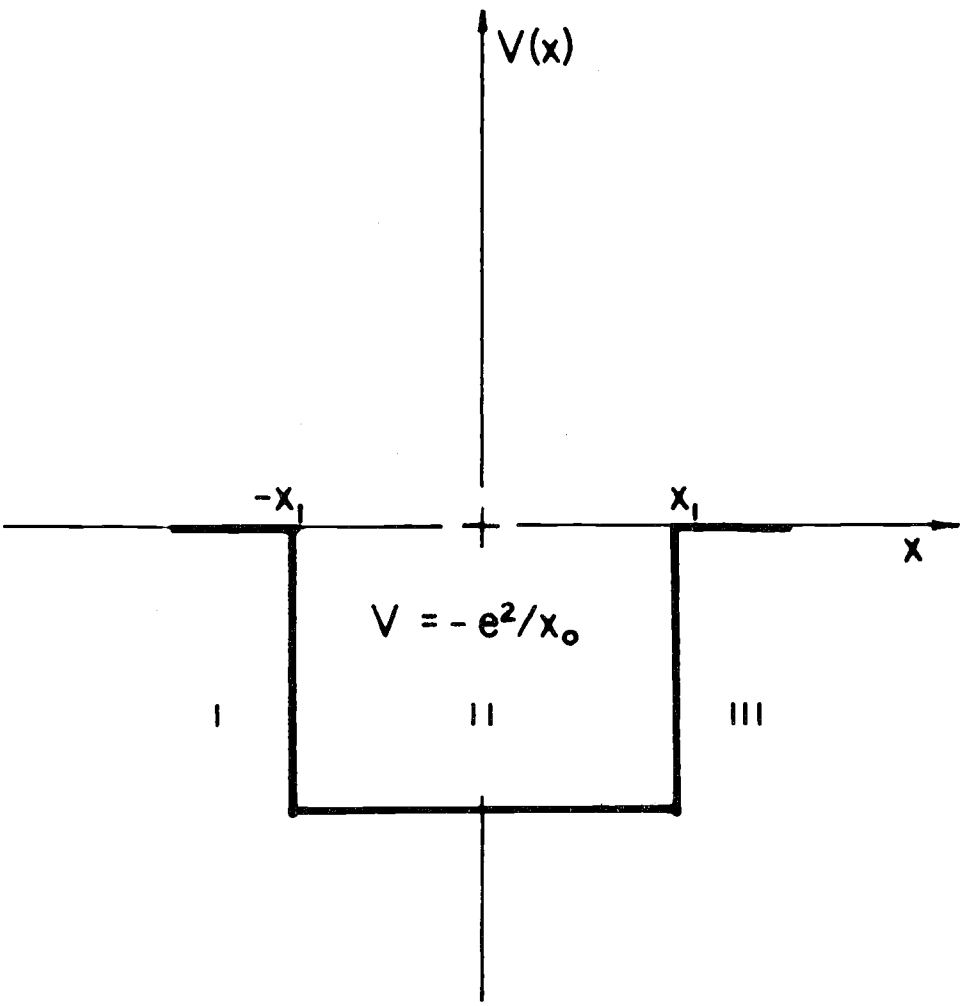

Figure 1. Diagram of a finite potential well.

$$\psi_I'' + k(E)\,\psi_I = 0$$

$$\psi_{II}'' + k(E + e^2/x_o)\,\psi_{II} = 0 \qquad [18]$$

$$\psi_{III}'' + k(E)\,\psi_{III} = 0$$

The respective general solutions of these equations are

$$\psi_I = A_1 e^{cx} + A_2 e^{-cx}$$

$$\psi_{II} = B_1 e^{idx} + B_2 e^{-idx} \qquad [19]$$

$$\psi_{III} = C_1 e^{cx} + C_2 e^{-cx}$$

where $c = \sqrt{-kE}$, $d = \sqrt{k(E + e^2/x_o)}$, and A, B, and C are arbitrary constants. When $E < 0$, corresponding to a bound state of the particle, c is real. This requires that A_2 and C_1 be set equal to zero in order that $\psi(x)$ remain finite in regions I and III. The resulting solutions of equations [18] are then

$$\psi_I = A_1 e^{cx} \qquad \psi_{III} = C_2 e^{-cx}$$

$$\psi_{II} = B_1 e^{idx} + B_2 e^{-idx} \qquad [20]$$

The Internuclear Potential

Derivation from the wave equation

When applied to a system of hydrogen-like molecules, the use of perturbed atomic delta-functions leads to a satisfactory solution of equation [16] and to the development of an internuclear potential function

applicable to hydrogen bonding. The delta-function is so defined that

$$\delta(x) = 0, \; x \neq 0 \qquad \delta(x) = \infty \;, \; x = 0 \qquad [21]$$

The function may be considered in the following exposition to be the limiting form of a finite square-well potential with increasing depth and decreasing width such that the product of the two dimensions remains finite and equal to g, the "strength of the delta-function."

Two assumptions concerning molecular bonds are required in applying the delta-function. They are:

1. Bond formation results from the coalizing of two shifted atomic delta-functions, of the appropriate separated-atom energies, into a molecular delta-function, in which the atomic delta-functions are located at the nuclear positions of the binding atoms when the internuclear distance is the equilibrium bond length.

2. The interatomic attraction and internuclear repulsion may be implicitly allowed for by the shifts of the delta-functions from the nuclear positions, with the result that the total energy of the system may be identified with that obtained from solving the wave equation [16] for the proposed model of chemical bonding.

The net effect of these assumptions, which are arbitrary but justifiable in terms of the results obtained, is that the delta-function spacing, a (a is the well center spacing which, when $x_o \to 0$, becomes the delta-function spacing), is less than r, the internuclear distance,

for stretched bonds; it is greater than r for compressed bonds, and is equal to r when the bond has its equilibrium length (see figure 2).

For the two-electron system shown in figure 2, the wave equation in one dimension is

$$\psi_1'' + \psi_2'' + k(E - V_1 - V_2)\psi = 0 \quad [22]$$

where the subscripts refer to the respective electrons 1 and 2 in regions II and IV, and V_1 and V_2 are the respective potential energies, $-e^2/x_o$, of the electrons. Assuming that $\psi = \psi(1)\,\psi(2)$, equation [22] becomes

$$\begin{aligned} \psi''(1) + k(E_1 - V_1)\psi(1) &= 0 \\ \psi''(2) + k(E_2 - V_2)\psi(2) &= 0 \end{aligned} \quad [23]$$

For simplicity the first of equations [23] will be solved and developed, to be combined later with the similar solution of the second of equations [23], thus giving the desired internuclear potential function. Referring to equations [20], the solutions for the various regions in figure 2 are[8]

$$\psi_I = A_I e^{c_1 x} \qquad \psi_{II} = D_{II} \cos d_1 x \qquad [24]$$

$$\psi_{III} = A_{III}(e^{c_1 x} + e^{-c_1 x}) \qquad \psi_{IV} = D_{IV} \cos d_1 x \qquad \psi_V = A_V e^{-c_1 x}$$

---

[8] ψ_{II} and ψ_{IV} are obtained from the definition $2\cos d_1 x = e^{id_1 x} + e^{-id_1 x}$.

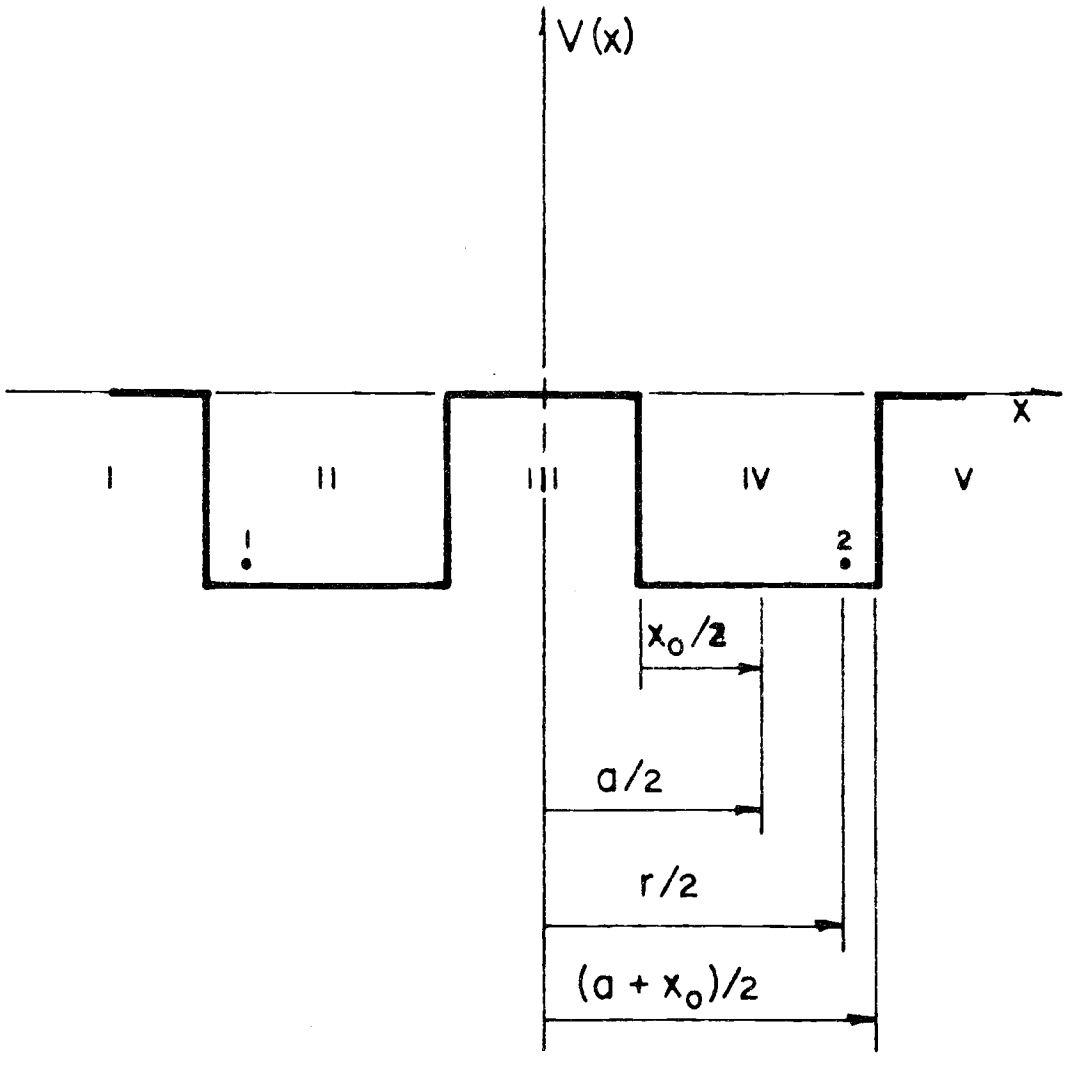

Figure 2. Diagram of potential wells before the formation of molecular delta-functions.

where, as before, $c_1^2 = -kE_1$, $d_1^2 = k(E_1 + e^2/x_o)$, and A and D are constants. The spin wave functions have not been included here, but can be if desired, since the wave equation is separable into spin and orbital wave equations (46, p. 355). The boundary conditions for the system pictured in figure 2 are

$$\text{at } x = -(a + x_o)/2 \qquad \psi_I = \psi_{II} \qquad \psi_I' = \psi_{II}'$$

$$\text{at } x = -(a - x_o)/2 \qquad \psi_{II} = \psi_{III} \qquad \psi_{II}' = \psi_{III}' \qquad [25]$$

$$\text{at } x = (a + x_o)/2 \qquad \psi_{IV} = \psi_V \qquad \psi_{IV}' = \psi_V'$$

$$\text{at } x = (a - x_o)/2 \qquad \psi_{III} = \psi_{IV} \qquad \psi_{III}' = \psi_{IV}' \qquad [26]$$

By the symmetry of the problem, the constants A_I, A_{III}, and A_V are equal, as are D_{II} and D_{IV}, and the conditions [25] are equal to conditions [26]. From the first of conditions [25] the relation

$$d_1/c_1 \tan d_1 (a + x_o)/2 = 1 \qquad [27]$$

can be formed. Similarly, using the second of conditions [25], the result

$$d_1/c_1 \tan d_1(a-x_o)/2 = \frac{e^{-c_1(a-x_o)/2} - e^{c_1(a-x_o)/2}}{e^{-c_1(a-x_o)/2} + e^{c_1(a-x_o)/2}} \qquad [28]$$

follows. The identity involving the tangent of a sum or difference of two angles reduces [27] and [28] to

$$\frac{d_1/c_1\ [\tan (d_1\, a/2) + \tan (d_1\, x_o/2]}{[1-\tan (d_1\, a/2)\ \tan (d_1\, x_o/2)\ ]} = 1 \qquad [29]$$

and

$$d_1/c_1\ \frac{[\tan (d_1\, a/2) - \tan (d_1\, x_o/2)\ ]}{[1 + \tan (d_1\, a/2)\ \tan (d_1\, x_o/2]} = \frac{1 - e^{c_1(a-x_o)}}{1 + e^{c_1(a-x_o)}}. \qquad [30]$$

Since $d_1^{\,2} = k(E_1 + e^2/x_o)$ and $\lim_{x_o \to o} d_1^{\,2}\,(x_o/2) = ke^2/2$, the formation of the molecular delta-function ($x_o/2 \to 0$) brings equations [29] and [30] into the form

$$(d_1/c_1)\ \tan d_1 a/2 + ke^2/2c_1 = 1 \qquad [31]$$

$$(d_1/c_1)\ \tan d_1 a/2 - ke^2/2c_1 = 1 - e^{c_1 a}/1 + e^{c_1 a} \qquad [32]$$

if the series approximation for $\tan d_1 x_o/2$ is used.[9] Subtraction of [31] from [32] yields

$$-ke^2/c_1 = -1 + (1 - e^{c_1 a} / 1 + e^{c_1 a}) \qquad [33]$$

or

$$c_1 = me^2 / \hbar^2(1 + e^{-c_1 a}) \qquad [34]$$

---

[9] For this approximation, $d_1 x_o/2 \ll \pi/2$, which is reasonable.

remembering that $k = 2m/\hbar^2$. In precisely the same manner the equality

$$c_2 = (me^2/\hbar^2)(1 + e^{-c\,a}) \qquad [35]$$

is obtained from solving the second of equations [23] and applying conditions [25]. Since $c^2 = -2mE/\hbar^2$, equations [34] and [35] can be combined to give

$$E = E_1 + E_2 = -(c_1^2 + c_2^2)\hbar^2/2m. \qquad [36]$$

The problem may be reduced to a consideration of the one-electron case through the reasonable assumption

$$c(\text{molecule}) = (c_1^2 + c_2^2)^{1/2} = \sqrt{2}\,c(\text{molecule-ion}). \qquad [37]$$

This is equivalent to putting the equation [22] into the form

$$\psi'' + k\,(E + g[\delta(x-a)/2 + \delta(x+a)/2]\,\psi = 0 \qquad [38]$$

where $\delta(x-a)/2$ and $\delta(x+a)/2$ are the appropriate delta-functions.[10] The one-electron wave functions for the bound states where $x \neq 0$ follow as

$$\begin{aligned} \psi &= Ae^{cx} && x < -a/2 \\ \psi &= A(e^{-cx} + e^{cx}) && -a/2 < x < a/2 \\ \psi &= Ae^{-cx} && x > a/2 \end{aligned} \qquad [39]$$

---

[10] A more complete discussion of this equation is given in the article by A. A. Frost entitled Delta-function model. I. Electronic energies of hydrogen-like atoms and diatomic molecules, to be found in J. Chem. Phys. 25:1150-54, 1956.

for the various regions of figure 2 which have coalesced to form regions similar to those in figure 1. It can be seen from these solutions that the energy state of the hydrogen-like molecule will be correctly given by the value of E.

From equation [37] it follows that

$$c(\text{molecule}) = 2\,(me^2/\hbar^2)\,(1 + e^{-c(\text{mol.-ion})a}) \qquad [40]$$

and that

$$E(\text{molecule}) = -\,(me^4/\hbar^2)\,(1 + 2e^{-ca} + e^{-2ca}). \qquad [41]$$

When $a \to \infty$, the molecular energy state given by equation [41] is the hydrogen-like atom energy. Since such a step is to be identified with $r \to \infty$, the potential function [41] behaves well at large r. At small r, the delta-function spacing, a, may be expanded in powers of r_e/r, where r_e is the unperturbed r:

$$a = r(b_o + b_1 r_e/r + b_2 r_e^2/r^2 + \dots)\,. \qquad [42]$$

For the value of a to be equal to r at large r, b_o must be unity. Since the delta-function spacing must also be r at small r (r near r_e) the values of b_1 and b_2 must appropriately be chosen as -1 and 1, respectively.

Neglecting the term e^{-2ca} in equation [41] as much smaller than $2e^{-ca}$, the potential function [41] is then given in terms of r by

$$E(r) = -me^4/\hbar^2\,(1 + 2e^{-cr_e} - c\Delta r^2/r) \qquad [43]$$

where $\Delta r = r - r_e$. Changing the energy scale by adding $me^4/\hbar^2$, and setting $(2me^4/\hbar^2) \exp(-cr_e)$ equal to D_e, one may derive the potential function

$$E(r) = - D_e \exp(-n\Delta r^2/2r) \qquad [44]$$

where D_e is the bond dissociation energy of a hydrogen-like molecule, and $n = 2c$.

Application to linear hydrogen bond systems

The potential function derived as equation [44] may be rewritten as

$$V(r) = D_e [1 - \exp(n\Delta r^2/2r)] \qquad [45]$$

where $n = k_e r_e/D_e$,[11] r is the internuclear distance, and k_e is the bond stretching force constant. In this case, the potential energy of the system is zero when r equals r_e, whereas the energy predicted by equation [44] is that referred to the dissociation energy as the "zero energy state."

Figure 3 is a diagram of a linear hydrogen bond system simplified to one dimension. Six assumptions shall be made in order to present a tractable problem:

---

[11] Found from the condition $d^2E/dr^2 = k_e$ when $r = r_e$, applied to equation [44].

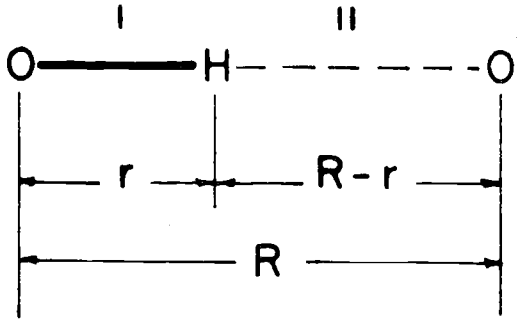

$$\Delta r_I = r - r_e$$

$$\Delta r_{II} = R - r - r_e^*$$

Figure 3. Diagram of a one-dimensional linear hydrogen bond.

1. The hydrogen atom is constrained to move only along the line of centers between the two electronegative atoms making up the bond.

2. Bond I in figure 3 is equivalent to a slightly stretched typical covalent bond, the amount of stretching being $r - r_e$, where r_e is the unperturbed internuclear distance.

3. Bond II is a weak, highly-stretched bond, the amount of stretching being $R - r - r_e^*$.

4. The Van der Waals repulsion between the two electronegative atoms can be described by an exponential function, Ae^{-bR}.

5. The electrostatic potential between the two electronegative atoms can be represented as $- B/R^m$, where B and m are constants.

6. The potential energy state of the two bonds may be described by a potential function having the form of equation [45].

The consequence of these assumptions is that the hydrogen bond is pictured as made up of two resonance structures:

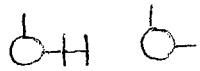

I

a valence bond

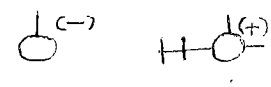

II

a covalent hydrogen bond

The model should be more accurate for crystalline rather than for liquid hydrogen bonds owing to the simple equations used to describe the internuclear attraction and repulsion energies.

The system in figure 3 is to be described by a potential function that contains four terms and, for convenience, goes to zero when R becomes infinite:

$$V = V_1 + V_2 + V_3 + V_4 \qquad [46]$$

where

$$V_1 = D_e [1 - \exp (-n(r-r_e)^2/2r)] \qquad [47]$$

$$V_2 = - D_e^* \exp (-n^* (R-r-r_e^*)^2 /2(R-r) \qquad [48]$$

$$V_3 = Ae^{-bR} \qquad V_4 = - B/R^m \qquad [49]$$

The equations [49] are combined using the definition

$$\lim_{R \to R_e} V_3 + V_4 = V_e \qquad [50]$$

where R_e is the equilibrium R, giving

$$V_3 + V_4 = V_e[2\exp(-b(R-R_e) - (R_e^m/R^m))] \qquad [51]$$

and making the constant coefficients of equations [49]

$$A = 2V_e e^{bR_e} \qquad B = V_e R_e^m \qquad [52]$$

Dividing B by A and substituting the result into equations [49], the relation

$$V_3 + V_4 = A [e^{-bR} - 1/2 (R_e/R)^m e^{-bR_e}] \qquad [53]$$

is obtained. The complete potential function is finally

$$V = D_e [\ 1-\exp(-n(r-r_e)^2/2r)\ ] - D_e^* \exp[\ (-n(R-r-r_e^*)^2/2(R-r)\ ]$$
$$+ A[\exp(-bR) - 1/2\ (R_e/R)^m \exp(-bR_e)\ ]. \qquad [54]$$

For the system pictured in figure 3, the following equilibrium conditions apply

$$\left(\frac{\delta V}{\delta r}\right)_{eq} = 0 \qquad \left(\frac{\delta^2 V}{\delta r^2}\right)_{eq} = K_H \qquad [55]$$

$$\left(\frac{\delta V}{\delta R}\right)_{eq} = 0 \qquad \left(\frac{\delta^2 V}{\delta R^2}\right)_{eq} = K_{O \ldots O} \qquad [56]$$

where k_H is the force constant associated with the hydrogen atom motion, and $k_{O \ldots O}$ is the constant associated with the motion of the oxygen atoms.

The model can predict internuclear distances, stretching frequencies of the OH radical, and hydrogen bond dissociation energies if the constants pertaining to bond II in figure 3 are evaluated as

$$n^* D_e^* = nD_e \qquad n^* = gn \qquad r_e^* = r_e \qquad [57]$$

where g is an empirical constant.

From equations [54] and the first of equations [55], the relation between r and R is found to be

$$r-r_e = \frac{\exp(-n^*(R-r-r_e^*)^2/2\ (R-r)\ (r^2(R-r-r_e^*)\ (R-r+r_e^*)}{\exp(-n\ (r-r_e)^2/2r)\ (R-r)^2\ (r+r_e)} \qquad [58]$$

The method of successive approximations is used to evaluate r for various values of R in equation [58]. Lippincott and Schroeder (30) give a table of R and r values obtained in this way which, because of the time-consuming method needed to evaluate equation [53], has been used in making the calculations in this investigation.

Assuming the molecules having the resonance structures shown previously to behave as harmonic oscillators when R is near R_e, the respective force constants are given by

$$k_{H_e} = 4\pi^2 \mu \omega_e^2 c^2 \qquad k_H = 4\pi^2 \mu \omega_H^2 c^2 \qquad [59]$$

where ω_H and ω_e refer to the hydrogen-bonded and free OH stretching frequencies in $cm.^{-1}$. From equation [54] and second of equations [55], the result

$$\omega_H/\omega_e = \left\{ \exp\left(-n(r-r_e)^2/2r\right) \frac{r_e}{r^3} \left[r_e^2 - n(r-r_e)^2 (r+r_e)^2/4r\right] + \exp\left(-n^*(R-r-r_e^*)^2/2(R-r)\right) \left(\frac{r_e^*}{(R-r)^3}\right) \left[r_e^{*2} - n^*(R-r-r_e^*)^2 (R-r+r_e^*)^2/4(R-r)\right] \right\}^{1/2} \qquad [60]$$

is obtained giving the dependence of the bonded stretching frequency upon the internuclear distance.

The dependence of the hydrogen bond dissociation energy upon the internuclear distance is specified when the bonded and unbonded stretch frequencies are known, and the empirical data are incorporated

into equations [60] and [54]. The constant A in equation [54] is evaluated, using known equilibrium distances, as

$$A = \frac{n^* D_e^*}{2}\left[1 - \frac{r_e^*}{(R_e - r)}^2\right]\left[\exp(-n^*(R_e - r - r_e^*)^2 / 2(R_e - r)\right]\left[\exp(-bR_e)\,(b - 1/2\,R_e)\right] \qquad [61]$$

from the first of equations [56], setting m equal to unity in agreement with resonance structure II where the two oxygen atoms carry partial charges.

The hydrogen bond dissociation energy given by equation [54] does not include the required contribution from the "zero-point" energy a bond possesses at the absolute zero of temperature nor does it apply for bonds at temperatures greater than absolute zero. A zero-point energy correction is simple to calculate if the stretching frequency of the bond is known since

$$E_o = 1/2\ hc\omega_o \qquad [62]$$

where E_o is the zero-point energy to be added to equation [54], h is Planck's constant, c is the speed of light <u>in vacuo</u>, and ω_o is the stretching frequency of the bond in $cm.^{-1}$ (46, p. 72). The temperature correction term, however, presents a more difficult problem. A general equation for the molar internal energy at any temperature is

$$u(T) = u_o + \int_o^T c_v(T)\,dT \qquad [63]$$

where u_o is the molar internal energy at absolute zero and c_v is the molar heat capacity at constant volume. Because the internal energy at 0° K. is entirely potential energy, u_o is equal to V in equation [54] plus E_o. The integral term, which accounts for the increases in the translational, rotational, vibrational, and electronic degrees of freedom, tends to increase the internal energy, with the result that the absolute value of u_o (since it is negative) is greater than u(T). This behavior is also what would be expected for a potential function and, therefore, is the basis for adding the integral term to equation [54] as a temperature correction.

The easiest method of evaluating equation [63], apparently that used by Lippincott and Schroeder (30), is to assume that the molecules making up the hydrogen bond dissociate into ideal monatomic gas molecules and that c_v is independent of temperature. Equation [63] can then be rewritten

$$u(T) = u_o + 3RT/2 \qquad [64]$$

since $c_v = 3R/2$. However, equation [64] is not too satisfactory an approximation for two reasons. First, the substance in question may not actually be a gas, certainly not an ideal gas, at the temperature T. Instead, it may have molecules in it which dissociate into a liquid or even a solid phase. If this were true, then equation [64] would give too high a value for u(T), since the heat capacity of a solid approaches 3R.

Second, it is an oversimplification to assume that c_v is temperature-independent when in fact it decreases with decreasing temperature, vanishing at absolute zero. This fact would lead to equation [64] giving a low u(T). Because of these limitations, the correction term 3RT/2 has not been used in calculating the dissociation energies reported in this thesis although, as a matter of fact, the effects of the two assumptions mentioned above are partially compensatory; rather, the values of c_v for the substance in question have been plotted against T from absolute zero to the desired temperature and the resulting curve integrated graphically. The expression used to obtain c_v for the solid phase was

$$c_v = 36R \left[\left(\frac{T}{\theta} \right)^3 \int_0^{\theta/T} \frac{x^3 \, dx}{e^{x-1}} - 1/4 \, \frac{\theta/T}{e^{\theta/T-1}} \right], \quad [65]$$

the Debye equation for the molar heat capacity of a monatomic crystal (60, p. 266), where θ is the Debye temperature (315° K. for ice), x is $hc\omega/kT$, k is Boltzmann's constant, and R, T, h, c, and ω have their previous significance. The Debye equation gives an accurate estimation of the molar heat capacity of a substance so long as it remains a solid and behaves approximately like a monatomic crystal. Because the freezing point of adsorbed water is variable and its Debye temperature is knknown, the hydrogen bond dissociation energies given for it in this thesis were temperature-corrected using the calculated heat capacities of ice as a reasonable approximation.

Empirical test of the hydrogen bond theory[12]

Any theory of molecular behavior is only as good as its predictive ability. It would be unreasonable to expect good results from applying Lippincott and Schroeder's theory to adsorbed water without first testing its validity with a variety of hydrogen-bonded crystals whose structures are well known. A determination of the mean systematic error of preduction through the comparison just suggested would provide a region of validity for the theory and allow a systematic error for the calculated properties of adsorbed water to be set.

The simplest test of the theory is a test of equation [60] which gives the hydrogen-bonded vibrational frequency as a function of the internuclear distance. These properties have been measured for many compounds and a good compilation of them is available. Figure 4 is a graph of the ratio of hydrogen-bonded to free OH stretching frequency for several compounds plotted against their respective hydrogen bond lengths. The lines extending horizontally from the data points represent

---

[12] The semiempirical theory of the hydrogen bond which has been presented here can be and has been criticized for the functions used in estimating repulsion and attraction energies and for the resonance model of chemical bonding it proposes. (See, for example, pp. 373-74 in Hydrogen Bonding, D. Hadzi, ed., Pergamon Press, New York, 1960.) However, in view of the fact that it is acknowledged that no better empirical treatment of the hydrogen bond exists (48, p. 238), it seems more worthwhile to test the theory on the basis of its predictive ability rather than its quantum-mechanical significance.

Figure 4. Observed and calculated dependence of ω_H/ω_e on R, the internuclear distance between hydrogen-bonded molecules.

Compound	R	ω_H/ω_e		Point No.
	Angstroms	Obs.	Calc.	
α - Resorcinol	2.66	0.716	0.776	1
Succinic Acid	2.64 ± 0.04	0.724	0.754	2
Adipic Acid	2.68	0.750	0.797	3
α - Iodic Acid	2.686 ± 0.009	0.751	0.802	4
Pentaerythritol	2.69	0.794	0.806	5
Diaspore	2.71 ± 0.05	0.802	0.824	6
Quinhydrone	2.71	0.826	0.824	7
Formic Acid	2.73 ± 0.05	0.832	0.839	8
Acetic Acid	2.76 ± 0.06	0.845	0.859	9
Boric Acid	2.72	0.865	0.832	10
Ice	2.76	0.876	0.865	11
$(COOH)_2 \cdot 2H_2O$	2.88 ± 0.02	0.935	0.929	12

The data are taken from Nakamoto, K., Margoshes, M., and Rundle, R. E. Stretching frequencies as a function of distances in hydrogen bonds. J. Am. Chem. Soc. 77: 6480-86, 1955.

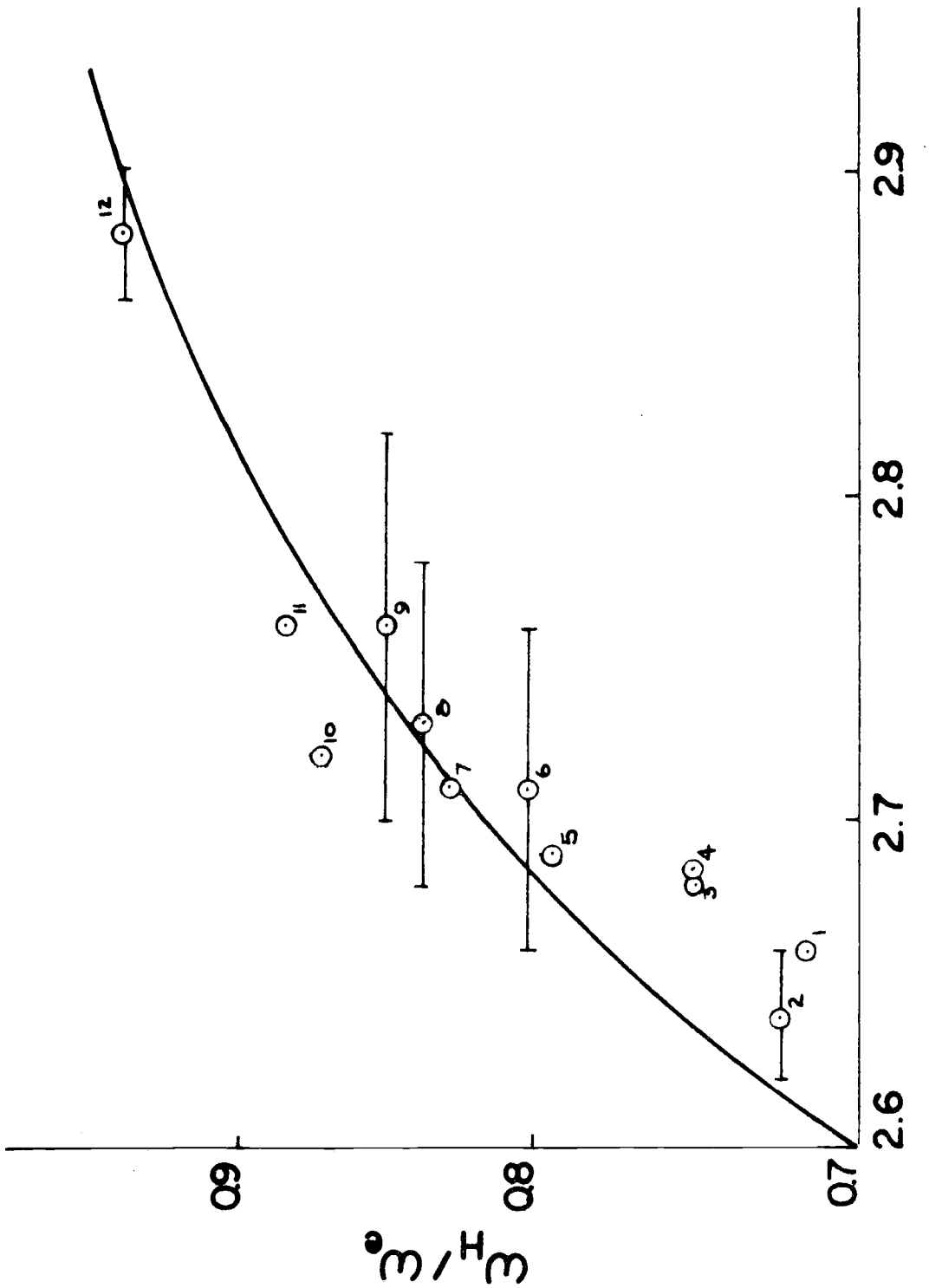
ω_H/ω_e
0.9
0.8
0.7
2.6
2.7
2.8
2.9
R in angstroms
1
2
3
4
5
6
7
8
9
10
11
12

the experimental errors. Equation [60] has been superimposed for comparison, using the following values for the constants. The numbers in parentheses refer to the sources of the empirical data.

$r_e = 0.97 \times 10^{-8}$ cm. (24, p. 489) $\quad n = 9.18 \times 10^8 \text{cm.}^{-1}$

$D_e = 118.2$ kcal. per mole (14) $\quad n^* = 13.32 \times 10^8 \text{cm.}^{-1}$

$D_e^* = 81.46$ kcal. per mole $\quad g = 1.45$

The value of D_e^* was calculated with equations [57], while the magnitudes of n and n^* were found from their definitions. The constant g has the value suggested by Lippincott and Schroeder (30). Each calculated ratio ω_H / ω_e was based upon a ω_e value of 3700 cm.^{-1} except for ice, whose ω_e value is known to be 3715 ± 10 cm.^{-1} (20, 55).

Agreement between the calculated and observed ratios ω_H / ω_e is good, the mean systematic error of prediction being 3.23 per cent of the observed values. However, the equation [60] does not seem to have the correct curvature in the region $R < 2.69$ A. One may reasonably wonder why a one-dimensional hydrogen bond theory gives any agreement with experiment. This is because it deals only with the stretching mode of the bonded hydroxyls, which is essentially a one-dimensional phenomenon and, therefore, is adequately treated by the theory.

It is worthwhile to test the theory in detail for ice, since this compound may have a direct bearing upon the adsorbed water structure.

Because R and r have been very accurately determined for this crystal, they are logical criteria for proving the theory. Lonsdale (31) gives the internuclear distance for ice at 0° C. as 2.760 A. for the hydrogen bonds parallel to the c-axis. Using this number, one obtains from equation [58] the r value 1.006 A. The observed value, according to Peterson and Levy (47), is 1. 011 $\pm$ 0.009 A. in good agreement with the theoretical value. With equation [60], one may predict the bonded hydroxyl stretch frequency for ice to be 3213 cm.$^{-1}$, using the calculated r value and 3715 cm.$^{-1}$ for ω_e. The experimental value of ω_H is 3256 cm.$^{-1}$ for ice at 0° C. (17, 42). Again, the calculated and empirical figures are close.

The equations [54], [61], [62], and [63] allow the calculation of the hydrogen bond energy for ice at 0° C. Including the temperature correction (1.1 kcal. per mole) and that for the zero-point energy (0.3 kcal. per mole), the calculated hydrogen bond dissociation energy is 5.7 kcal. per mole.[13] The two experimental values given by Pimentel and McClellan (48, p. 214) are 5.75 and 6.6 kcal. per mole, while the theoretical values compiled by these authors range from 3.0 to 7.7 kcal. per mole. Pauling (45, p. 468) suggests 5.0 kcal. per mole. Based upon

---

[13] The magnitude of the empirical constant, b, in equation [61] was taken to be 4.8 x 10^8 cm.$^{-1}$ (30). The ground state of frequency, ω_o, in equation [62] was assumed to be 200 cm.$^{-1}$ (48, p. 134).

the comparisons made here, it appears that the theory of Lippincott and Schroeder gives a reasonable picture of the hydrogen bond in ice and, therefore, is adequate for application to adsorbed water on montmorillonite.

EXPERIMENTAL MATERIALS AND METHODS

Preparation of the Clay Films

The montmorillonite selected for study was a Wyoming bentonite obtained from the American Colloid Company under the name Volclay. This mineral is mined near Upton, Wyoming, and is known to be a nearly chemically-pure montmorillonite (28).

The clay powder was passed through an ASTM No. 300 Standard Sieve and ten grams of it were placed in suspension with 500 ml. of distilled water. Clay and water were mixed thoroughly for one hour with a Hamilton Beach blendor and then transferred to a 1000 ml. graduate cylinder. The cylinder was filled with distilled water to the liter mark and placed in a water bath where the temperature remained at 26.48 $\pm$ 0.01° C. Stokes' law was used to determine the settling time required to leave only the clay particles of less than 0.5 micron diameter in suspension. This time was 3.8 days for a settling distance of 37 cm.

After settling, the upper 500 ml. of suspension were decanted from the graduate cylinder and run through an Amberlite 120 cation exchange resin charged with either lithium, sodium, potassium, or

calcium ions. Subsequent chemical analyses showed that usually two passages at 100 ml. per minute were enough to insure complete exchange with the clay particles. The clay salts prepared in this way were expected to have only a minimal amount of Al- and Fe-hydroxy compounds and free silica present with them since very little lattice-destroying hydrogen ion was in the suspensions (see table 1). Each homoionic clay suspension was stored in a stoppered jar to await further treatment. After about two weeks of standing, the pH value of each suspension was measured with a Beckmann pH meter.

The excess salts present in the clay suspensions were removed by centrifugation at 2500 RPM for five minutes followed by decantation and redilution in deionized water. This was repeated until the supernatant gave no positive AgCl test; although no specific test for sulfate ions was performed, they were considered to be no more concentrated than the chloride ions and, therefore, were assumed removed when the latter were proven to be so.

Thin films of the clay suspensions were made by drying them on clean pieces of teflon in a dessicator containing $CaCl_2$. Additional drying of the films was accomplished by laying them over P_2O_5 for 2 to 5 days.

It was found desirable to prepare slightly hydrated films whose infrared spectra could be compared to those of the dry films. This was done by making the hydrated films in a sealed "dry box" in the presence

of a saturated solution of LiCl, which is known to produce a relative pressure of 0.15 at 20° C. (25, p. 2499). Although the temperature of the dry box was 25 ± 2° C. during the day, the relative pressure over the LiCl solution was still 0.15, as indicated by a calculation using the Clausius-Clapeyron equation.

Elaborate and time-consuming procedures are required if one wishes to know accurately the water contents of slightly hydrated clays. To avoid these operations while yet retaining some knowledge of the moisture content of the clay salts prepared for this investigation, a method of estimating water content based upon the desorption isotherms of Mooney et al. (41) was devised. Using the integrated form of the Clausius-Clapeyron equation and a latent heat of desorption value of 12 kcal. per mole (suggested by Mooney's data), the relative pressure at the temperature of Mooney's measurements giving the same water content as a relative pressure of 0.15 at 25° C. was found to be 0.141. The moisture contents of the clay films hydrated in the presence of LiCl thus were inferred from this relative pressure and Mooney's data. Changes in the water contents of the hydrated films after their removal from the dry box were attenuated by immediately transferring them to the infrared absorption cell and sealing it. Because the moisture contents of the clays were not particularly low (3-11 per cent), little adsorption of water vapor probably occurred during the transfer.

The moisture contents of the dried films were determined by comparing the integrated absorption, which has been shown to be proportional to the concentration of the absorbing substance (12), of the dried clay spectrum to that of the hydrated clay spectrum. By converting the relative per cent transmittances in the 3000 to 3900 $cm.^{-1}$ region[14] of the adsorbed water spectrum to absorbances and determining the area beneath the resulting absorbance curve with a suitable method (e.g., Simpson's rule, 25, p. 346), one may find the integrated absorption. The ratio of the integrated absorption of the dried film to that of the hydrated film, multiplied by the estimated water content of the latter, gives an estimate of the moisture content of the dried film.

The water content of each clay film used in this research was determined by one or the other of the methods just described. With two exceptions, each measurement was made in duplicate. The relative errors calculated for these data were usually small, indicating that the effects of temperature variations in the dry box, deviations from Beer's law, and changes in film thickness were mutually compensatory in most instances.

---

[14] The observed per cent transmittance divided by the per cent transmittance of the CaF_2 in the same region of the spectrum is the relative per cent transmittance. This quantity was used instead of the observed per cent transmittance so that the spectra of different clay films could be compared.

Chemical Analysis

No assumptions of homogeneity are warranted for clay salts prepared with exchange resins; chemical analyses are necessary to confirm their purity. For analyzing the clay films used in this research, emission spectrophotometry was picked for its convenience and simplicity.

Each clay salt was prepared for analysis by centrifugation at 2500 RPM followed by redilution with ethyl alcohol, as suggested by Jackson (26). When the supernatant gave no positive test for chloride or sulfate ions[15], the clay was resuspended in deionized water. Two 10 ml. aliquots of the purified clay suspension were each treated with equal volumes of normal NH_4OAc at pH 6.9 for periods ranging up to 24 hours, increasing with the charge and decreasing radius of the exchangeable cation. Two 5 ml. aliquots of the same suspension were saved for subsequent gravimetric analysis (oven dry basis) to determine its clay concentration. The treated clay was centrifuged after complete exchange, the supernatant then collected and analyzed immediately for the exchanged cation with a Beckmann DU flame photometer. Each determination was made in duplicate or triplicate.

---

[15] Because Ag_2SO_4 is insoluble in alcohol, the addition of $AgNO_3$ to the supernatant tested for both chloride and sulfate ions.

The per cent transmittances of the exchanged-cation solutions were converted to parts per million with standard curves prepared as recommended by Jackson (26). The me. cation per gm. clay were calculated by dividing the ion concentration by the clay concentration of the suspension chosen for analysis.

Infrared Analysis

The clay films were prepared for spectral analysis by inserting them between circular flourite windows, each 0.5 cm. thick, and using electrician's tape to hold the windows together and seal in the clay film. This operation was always carried out in an atmosphere of relative humidity near 15 per cent.

A simple device was designed to hold the windows and clay film in the infrared beam. It consisted of a semicircular aluminum trough fastened to a plate of the same metal and surmounted by a spring-clip which served to hold the CaF_2 windows securely in the trough. A hole one cm. in diameter drilled through the aluminum plate just above the trough allowed the passage of the infrared beam through the clay film in its sample holder.

Infrared spectra of the clay films were taken at about 25° C. with the Beckmann IR-4 spectrophotometer (NaCl optics). The instrument was adjusted before each determination as follows: coarse gain,

10; fine gain, 600; period, 8; slit width, 0.33 standard width; scanning speed, 0.5. Each run was made with an empty pair of CaF_2 windows in the reference beam. The single-beam spectrum of these windows is shown in figure 5. From the lack of absorption in the 3 micron region, one may conclude that no measurable amount of water was present on the windows.

Spectra of the homoionic films were taken in duplicate using different samples each time. In general, the noise level of the spectrophotometer was moderate, although some care was required to avoid confusing a real absorption peak with one caused by a random electrical fluctuation. Band centers in the 3 and 6 micron regions were measured from the recorded spectra with a Gerber variable scale,[16] an ingenious device that allows one to interpolate graphs of any scale from an expandable spring graduated in tenths. Deviations from the mean were computed and averaged for each reproducible band center.

---

[16] Manufactured by the Gerber Scientific Instrument Co., 89 Spruce Street, Hartford 1, Conn.

Figure 5. Infrared spectrum of the CaF_2 windows.

EXPERIMENTAL RESULTS

Properties of the Clay Films

The properties of the homoionic clay films studied, as determined by the methods just described, are listed in table 1. Estimated errors following the water content data are mean deviations. Although the relative mean deviation in the exchange capacity data may appear to be large, it is about the same as that to be found in the carefully taken exchange capacity data of Kerr et al. (28) for Upton, Wyoming, bentonite; evidently the errors reflect the heterogeneity of this clay.

Stretching Frequencies

The 3 micron infrared spectra of the water adsorbed by Li-, Na-, K-, and Ca-bentonite are shown in figures 6 and 7 superimposed for comparison upon a relative per cent transmittance scale. The band centers, which in the writer's judgment, best represent the absorption maxima are identified by arrows. Because the noise level in the IR-4 was moderately high in the 3 micron region, because the NaCl prisms in this instrument show the greatest dispersion in this region, and because the temperature at which the spectra were recorded (25° C.)

Table 1. Properties of the Clay Films Used in the Research.

Saturating Cation	Exchange Capacity	Suspension pH Value	Film Thickness	Moisture Content	
				Dry	Hydrated
	me./gm clay		mg./cm.[b]	mg. water/ gm. clay	
Li^+	0.94[a]	7.6[b]	1.6[c]	71 ± 1[d]	80[e]
Na^+	0.92	7.2	1.4	24 ± 2	54
K^+	0.91	7.3	1.7, 0.7	18 ± 3	30
Ca^{++}	0.93	6.9	2.1	70 ± 10	110

[a] Mean relative deviation ± 8.0%.

[b] Approximately 1% suspensions at 25° C.

[c] Determined by dividing the film weight, after spectral analysis, by the film area, measured with a polar planimeter. Mean deviation about ± 0.1 mg./cm.^{2} .

[d] Estimated from integrated absorption data.

[e] Estimated from the desorption data of Mooney et al. (41).

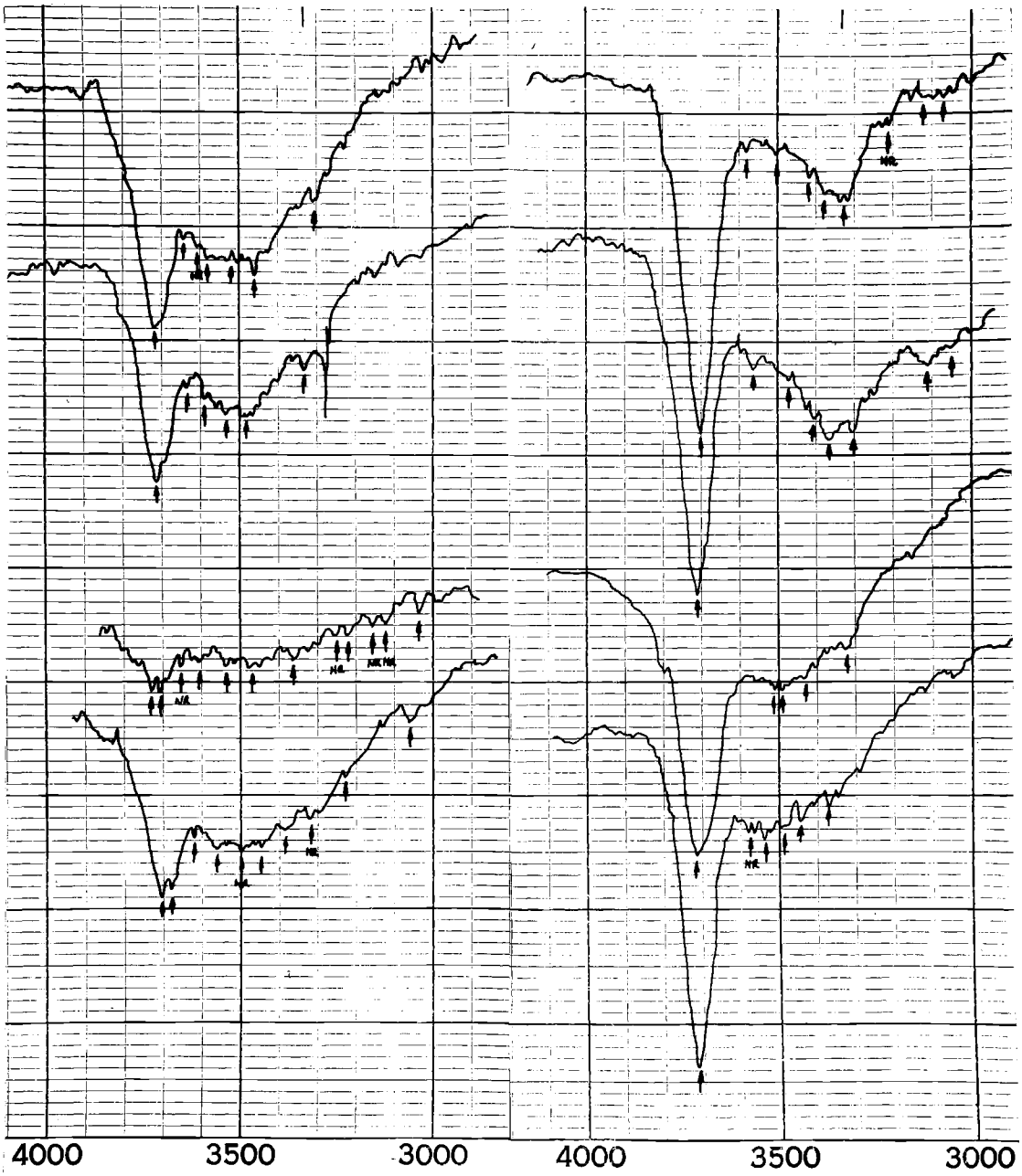

Figure 6. The 3 micron infrared spectra of the water adsorbed by Li-bentonite (on the left) and by Na-bentonite (on the right). Upper pairs of spectra are those for the dry clays, lower pairs are for the hydrated clays.

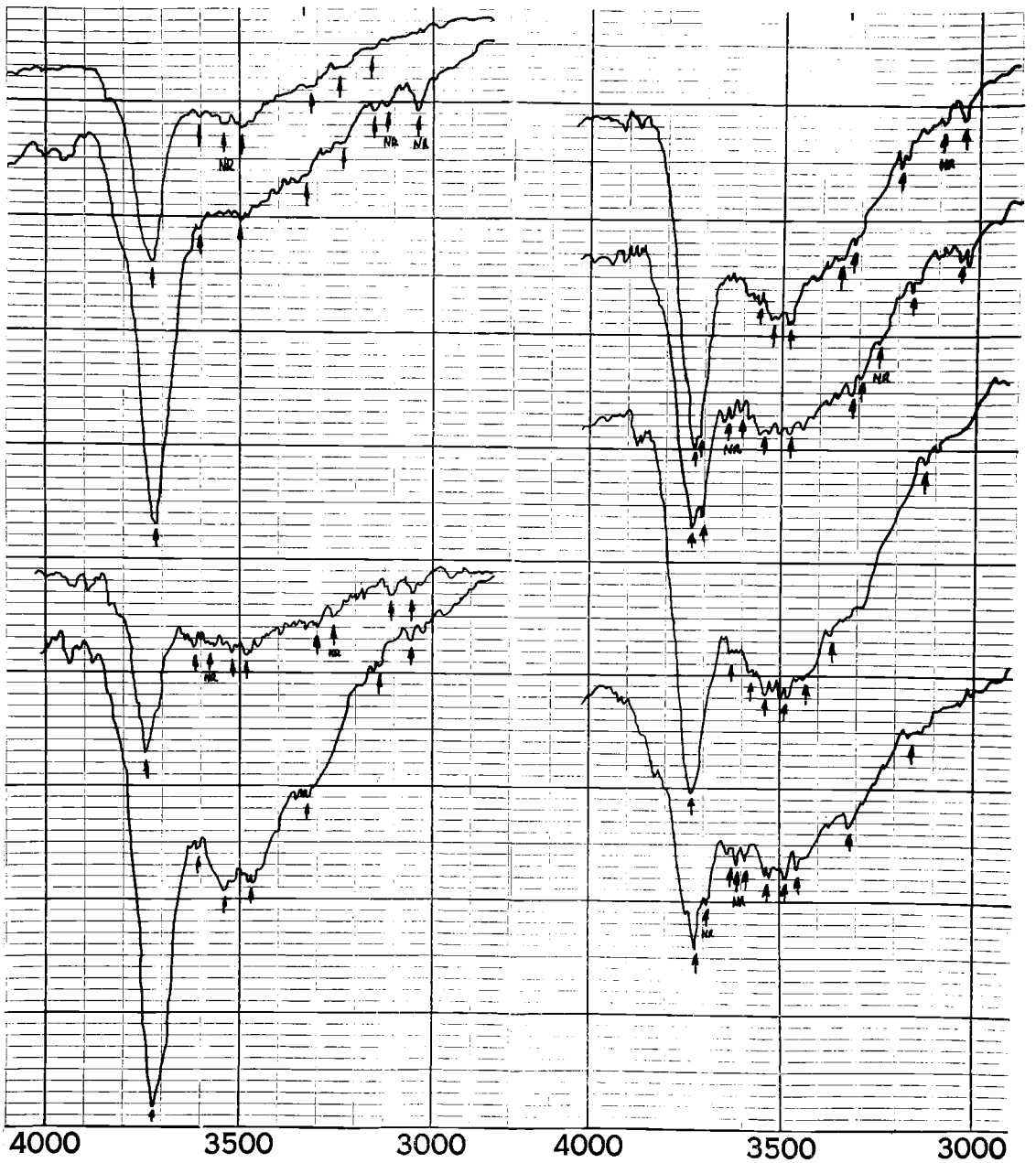

Figure 7. The 3 micron infrared spectra of the water adsorbed by K-bentonite (on the left) and by Ca-bentonite (on the right). Upper pairs of spectra are those for the dry clays, lower pairs are for the hydrated clays.

was not precisely controlled, some reasonable doubt as to the accuracy of these data may be expressed. However, in view of the fact that the IR-4 was carefully calibrated with a polystyrene standard so as to account for errors in the spectra due to optical dispersion, the fact that 86 per cent of all the chosen band centers were reproducible, and the fact that these spectra are the only ones for adsorbed water known to the writer which show more detail than just one broad absorption in the 3 micron region, one must at least concede that the data presented here represent a positive step toward getting an accurate spectral picture of the adsorbed water lattice.

Tables 2 through 5 list the mean stretching frequencies calculated from figures 6 and 7 and corrected for the + 1.67 per cent systematic error in the spectrophotometer. The data have not been corrected to vacuum conditions since this correction is much smaller than the experimental errors. Frequency assignments as to vibrational mode have been made through comparison of the data to that for water and ice (19, 42, 56).

Bending Frequencies

Figures 8 and 9 show the duplicate spectra for water on the clay films in the 6 micron region; tables 6 and 7 list the mean bending frequencies, corrected for a + 0.25 per cent systematic error in the

Table 2. Stretching Frequencies and Their Assignments for Water Adsorbed by Li-bentonite.

Dry Clay		Hydrated Clay	
Frequency, cm^{-1}	Mode	Frequency, $cm.^{-1}$	Mode
3655[a]	ν_3[b]	3647[c]	ν_3
3576	ν_3'	3627	ν_3
3524	ν_3'	3547	ν_3'
3467	ν_3	3482	ν_3'
3411	ν_3'	3391	ν_3'
3263	$2\nu_2$	3308	$2\nu_2$
		3163	ν_3'
		2985	ν_3'

[a] Mean deviation $\pm$ 6 $cm.^{-1}$. Systematic error correction -0.0167ν.

[b] Symbols:

ν_3 : unbonded OH assymetric stretch mode

ν_3' : hydrogen-bonded OH assymetric stretch mode

$2\nu_2$: combination of the OH bend mode, ν_2

[c] Mean deviation $\pm$ 8 $cm.^{-1}$.

Table 3. Stretching Frequencies and Their Assignments for Water Adsorbed by Na-bentonite.

Dry Clay		Hydrated Clay	
Frequency, $cm.^{-1}$	Mode	Frequency, $cm.^{-1}$	Mode
3642[a]	ν_3	3639[b]	ν_3
3506	ν_3'	3465	ν_3'
3426	ν_3'	3431	ν_3'
3352	$2\nu_2$	3374	$2\nu_2$
3311	ν_3'	3285	ν_3'
3249	ν_3'		
3069	ν_3'		
3012	ν_3'		

[a] Mean deviation $\pm$ 7 $cm.^{-1}$.

[b] Mean deviation $\pm$ 9 $cm.^{-1}$.

Table 4. Stretching Frequencies and Their Assignments for Water Adsorbed by K-bentonite.

Dry Clay		Hydrated Clay	
Frequency, cm.$^{-1}$	Mode	Frequency, cm.$^{-1}$	Mode
3657[a]	ν_3	3667[b]	ν_3
3541	ν_3'	3547	ν_3'
3439	ν_3'	3467	ν_3'
3262	$2\nu_2$	3416	ν_3'
3172	ν_3'	3249	$2\nu_2$
3089	ν_3'	3065	ν_3'
		3006	ν_3'

[a] Mean deviation ± 3 cm.$^{-1}$.

[b] Mean deviation ± 8 cm.$^{-1}$.

Table 5. Stretching Frequencies and Their Assignments for Water Adsorbed by Ca-bentonite.

Dry Clay		Hydrated Clay	
Frequency, cm.$^{-1}$	Mode	Frequency, cm.$^{-1}$	Mode
3657[a]	ν_3	3664[b]	ν_3
3637	ν_3	3568	ν_3'
3525	ν_3'	3524	ν_3'
3485	ν_3'	3472	ν_3'
3413	ν_3'	3419	ν_3'
3283	ν_3'	3389	ν_3'
3247	$2\nu_2$	3294	$2\nu_2$
3149	ν_3'	3097	ν_3'
2988	ν_3'		

[a] Mean deviation $\pm$ 6 cm.$^{-1}$.

[b] Mean deviation $\pm$ 5 cm.$^{-1}$.

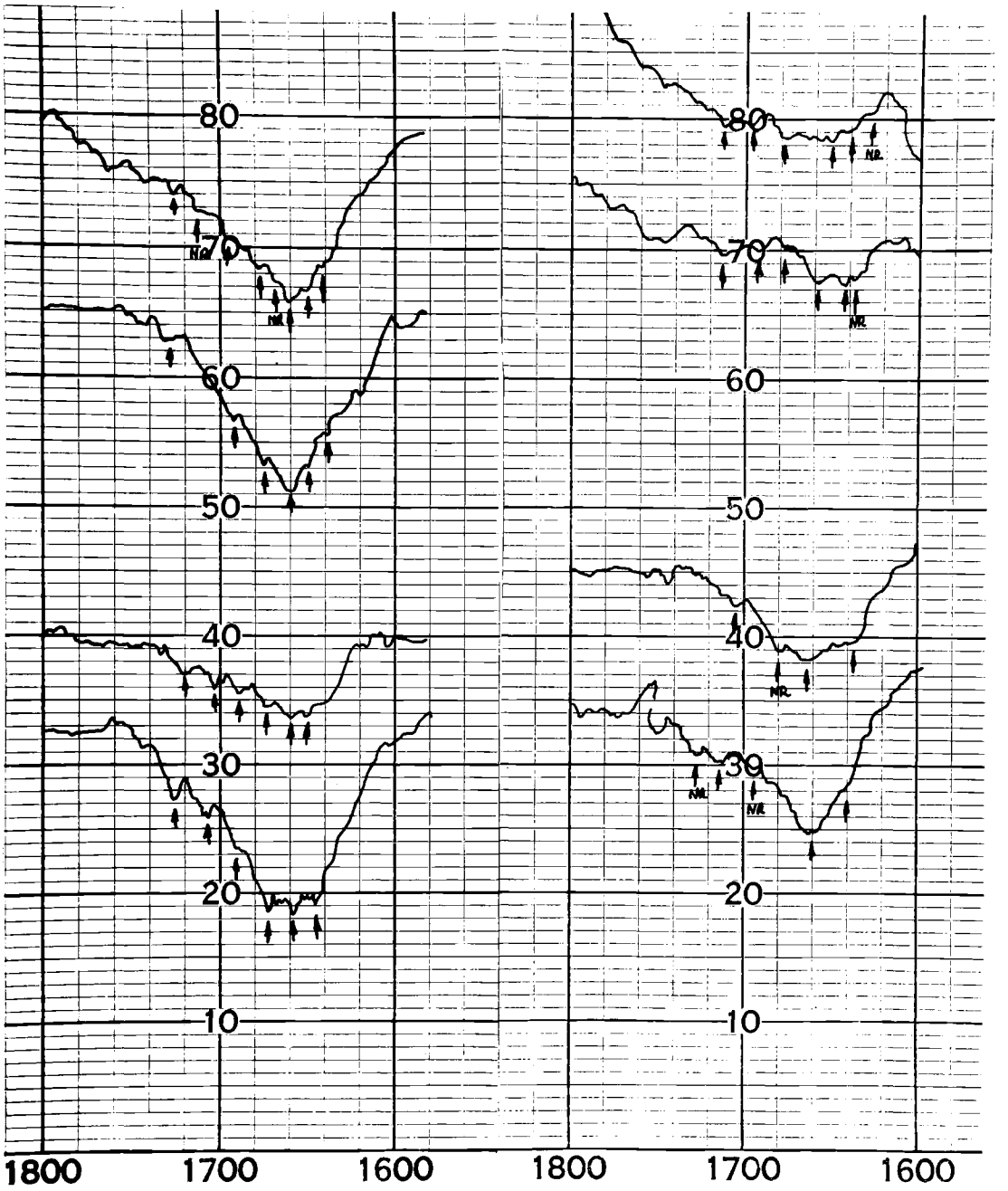

Figure 8. The 6 micron infrared spectra of the water adsorbed by Li-bentonite (on the left) and by Na-bentonite (on the right). Upper pairs of spectra are those for the dry clays, lower pairs are for the hydrated clays. The per cent transmittance numbers have no significance here as this scale is relative.

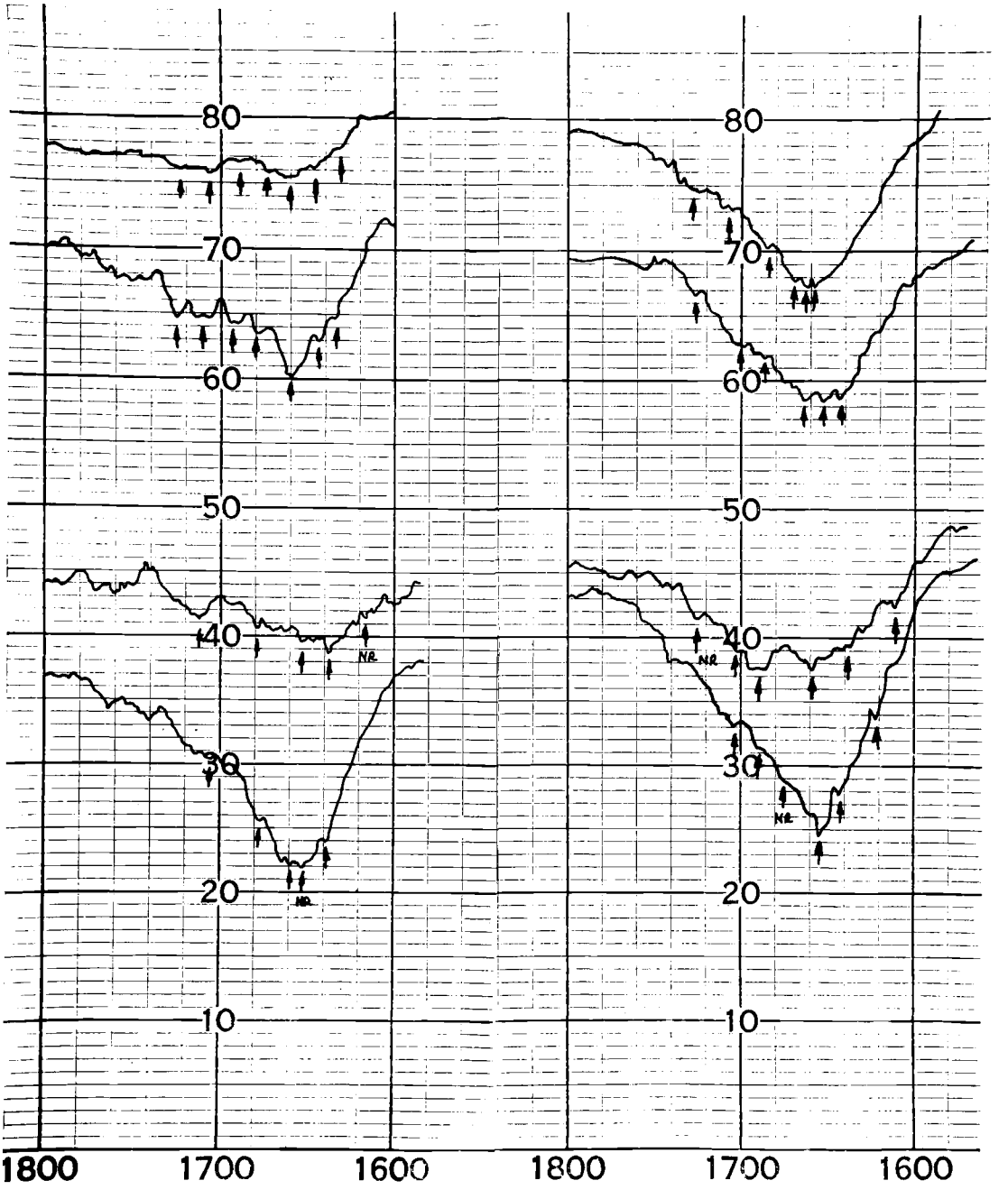

Figure 9. The 6 micron infrared spectra of the water adsorbed by K-bentonite (on the left) and by Ca-bentonite (on the right). Upper pairs of spectra are those for the dry clays, lower pairs are for the hydrated clays. The per cent transmittance numbers have no significance here as this scale is relative.

IR-4. Eighty-nine per cent of the chosen band centers were reproducible, probably reflecting the lower noise level of the spectrophotometer in the 6 micron region.

The absorption near 6 microns for water is associated with the in-plane bending vibration (48, p. 118 ff), a mode which often interacts with other skeletal motions of the water lattice (55). That this is also the case for the spectra of the adsorbed water lattices is shown by the following facts. An absorption at 53 $cm.^{-1}$ has been observed several times in the raman spectrum of ice (19, 42), while one at 60 $cm.^{-1}$ has been reported for water (19). These absorptions have been assigned as both the lattice translational motion frequency (42) and the in-plane bending frequency of the hydrogen bond (48, p. 68). The former assignment seems the more correct since the absorption frequencies, if related, shift in the wrong direction, with increased hydrogen bonding for a bending vibration, and show no isotopic shift (19). Applying this conclusion to the adsorbed water spectra, it seems reasonable that the higher absorption frequencies near 1600 cm^{-1} are combinations of the lower frequencies there with lattice translational modes that should absorb somewhere around 53 to 60 $cm.^{-1}$. Table 8 shows a test of this hypothesis using the spectral data for the dry clay films and the lattice translational motion frequencies for both ice and water. As can be seen, the agreement between the observed and predicted overtones is good.

Table 6. Bending Frequencies and Their Assignments for Water Adsorbed by Li- and Na-bentonite.

Li-bentonite			Na-bentonite		
Frequency[a]		Mode	Frequency		Mode
Dry	Hydrated		Dry	Hydrated	
1636[b]	1642[c]	ν_2	1633[d]	1634[e]	ν_2
1646	1655	ν_2	1649	1658	ν_2
1657		ν_2	1674		ν_2
1668	1669	ν_2	1690	1705	$\nu_2 + \nu_T$
1686	1687	$\nu_2 + \nu_T$	1708		$\nu_2 + \nu_T$
1726	1720	$\nu_2 + \nu_T$			
	1702	$\nu_2 + \nu_T$			

[a] Systematic error correction -0.0025ν.

[b] Mean deviation ± 1 cm.$^{-1}$.

[c] Mean deviation $\pm$ 2 cm.$^{-1}$.

[d] Mean deviation $\pm$ 2 cm.$^{-1}$.

[e] Mean deviation $\pm$ 2 cm.$^{-1}$.

Symbols: ν_2: in-plane OH bending mode

ν_T: lattice translational mode

Table 7. Bending Frequencies and Their Assignments for Water Adsorbed by K- and Ca-bentonite.

K-bentonite			Ca-bentonite		
Frequency		Mode	Frequency		Mode
Dry	Hydrated		Dry	Hydrated	
1630[a]	1634[b]	ν_2	1645[c]	1636[d]	ν_2
1641	1648	ν_2	1652	1652	ν_2
1656	1673	ν_2	1661	1612	ν_2
1671		ν_2			
1687		$\nu_2 + \nu_T$	1678	1687	$\nu_2 + \nu_T$
1704	1706	$\nu_2 + \nu_T$	1702	1700	$\nu_2 + \nu_T$
1720		$\nu_2 + \nu_T$	1724		$\nu_2 + \nu_T$

a Mean deviation $\pm$ 1 cm.$^{-1}$.

b Mean deviation $\pm$ 1 cm.$^{-1}$.

c Mean deviation $\pm$ 4 cm.$^{-1}$.

d Mean deviation $\pm$ 2 cm.$^{-1}$.

Table 8. Comparison of Observed and Predicted Combination Frequencies for the 6 μ Modes in Adsorbed Water.

Saturating Cation	Observed Fundamental	Predicted Overtones		Observed Overtone	ν_T
		$\nu_2 + 53$	$\nu_2 + 60$		
Li^+	1636[a]	1689	1696	1686	50
Li^+	1646	1699	1706	(1710)[b]	(64)
Li^+	1657	1710	1717	1726	69
Na^+	1633	1686	1693	1690	57
Na^+	1649	1702	1709	1708	59
K^+	1630	1683	1690	1687	57
K^+	1641	1694	1701	1704	63
K^+	1656	1709	1716	1720	64
Ca^{++}	1645	1698	1705	1702	57
Ca^{++}	1652	1705	1712	(1706)	(54)
Ca^{++}	1661	1714	1721	1724	63

[a] All data are reported in $cm.^{-1}$.

[b] Nonreproducible frequency included for completeness.

DISCUSSION

Water Adsorbed on Na-bentonite

The lengths and dissociation energies of the hydrogen bonds in the water adsorbed by Na-bentonite, calculated from the data in table 3, are given in table 9. In calculating the bond energies, the zero-point energy for ice (0.3 kcal. per mole) and a temperature correction to 25° C. (1.2 kcal. per mole) were used, the latter being made by the method described in the second part of the theory section using the calculated heat capacities for ice. However, the temperature correction term must be considered only approximate, since the internal degrees of freedom of the adsorbed water lattice vary with moisture content (34). For this reason the dissociation energies listed in tables 9 and 10 must be regarded as first-order estimates until the heat capacity of adsorbed water as a function of water content and temperature has been accurately determined.

The bond lengths in table 9 indicate that two different water structures are present on Na-clay at very low moisture contents. The 3.01, 2.92, 2.73, and 2.71 A. bonds may be considered to represent a

Table 9. Hydrogen Bond Lengths and Dissociation Energies in the Water Adsorbed by Na- and K-bentonite.

0.27 Monolayer Coverage[a]		0.60 Monolayer Coverage	
Bond Length A.	Bond Energy kcal./mole	Bond Length A.	Bond Energy kcal./mole
	Na-bentonite		
3.01	0.6	2.96	1.1
2.92	1.7	2.92	1.7
2.83	3.5	2.81	4.0
2.80	4.3		
2.73	6.7		
2.71	7.6		
0.23 Monolayer Coverage[b]		0.38 Monolayer Coverage	
Bond Length A.	Bond Energy kcal./mole	Bond Length A.	Bond Energy kcal./mole
	K-bentonite		
3.01	0.6	3.01	0.6
2.92	1.7	2.94	1.4
2.76	5.5	2.89	2.2
2.73	6.7	2.72	7.1
		2.71	7.6

[a] Estimated from table 1 and the x-ray data of Mooney et. al. (41).

[b] Estimated from table 1 and the BET data of Orchiston (43).

distorted version of the Hendricks-Jefferson structure; this conclusion necessarily implies the noninterference of the exchangeable cations, either through occlusion in the hexagonal cavities of the clay surface or isolation on widely scattered, high energy exchange sites. The 2.80 and 2.83 A. bonds, since they are very close in length to the mean hydrogen bond distance of 2.85 A. determined for the liquid water structure by x-ray and infrared methods (55), may be associated with liquid-like, two-dimensional hydration shells about the exchangeable cations. At 0.6 monolayer coverage, when diffusion of the Na ions apparently becomes possible, the data in table 9 indicate that the Hendricks-Jefferson structure is completely broken up in favor of a two-dimensional hydration structure having bond lengths characteristic of liquid water. Qualitatively, this may be seen in the shift of the 3 micron spectrum of Na-clay (figure 6), as its water content increases, from a discrete set of absorption bands around 3300 $cm.^{-1}$ (characteristic of ice) to a broader, less detailed absorption at 3500 $cm.^{-1}$ (characteristic of liquid water).

If the view just proposed is accepted, it follows that the water molecules on Na-bentonite should be in a transitory state at low coverage, resulting from competition between the clay surface and the exchangeable cations for hydration structures. Such behavior is evidenced by the fact that the BET theory does not describe water desorption on Na-bentonite until monolayer coverage is attained (41). One may

consider the deviation from theory the result of a variable monolayer water content or a transitoriness in the organization of the water molecules made apparent by a variability in the monolayer heat of desorption (E_1). Because the former cause implies a clay surface whose own structure changes with moisture content and the latter only that the arrangement of the water molecules on the surface changes significantly with moisture content, a variable monolayer heat of desorption seems the more probable. If the value of E_1 can be considered approximately equivalent to an enthalpy of desorption, the entropy of desorption may be calculated from the definition of the Gibbs free energy and the desorption isotherms of Mooney et al. (41) by calculating E_1 as a function of relative pressure (and, therefore, moisture content) using the BET equation (8). To do this one must assume a constant value of the monolayer water content; the value of 90 mg. water per gm. clay, indicated by the x-ray diffraction data of Mooney et al. (41), was chosen in this calculation. The resulting plot of the entropy of desorption versus monolayer coverage shows a nearly linear, gradual increase as the coverage increases from 0.2 to 0.8. Between 0.8 and 1.0 the entropy of desorption increases sharply, probably as the result of the coalescence of scattered hydration shells into an organized monolayer.

The average hydrogen bond dissociation energy for the water molecules at 0.6 monolayer coverage on Na-bentonite can be estimated

from the isosteric heat of desorption data of Mooney et al. (40) to be 5.6 kcal. per mole, assuming that the Van der Waal's attraction energy among the water molecules is 1.3 kcal. per mole[17] and, less reasonably, that the contribution to the heat of desorption from the heat of dehydration of the exchangeable Na ions is negligible. The calculated energy of the bonds of greatest number in the adsorbed water lattice at the same coverage (as estimated from the depth of the band centers shown in figure 6) is 4.0 kcal. per mole, in fair agreement with the value computed from desorption data considering the approximate nature of both calculations. That the value determined from infrared spectra is near the hydrogen bond energy of liquid water (4.6 kcal. per mole at 25° C.) is additional evidence for the conclusions drawn previously stressing the structural similarity of the water on Na-bentonite at low coverage and ordinary liquid water.

Water Adsorbed on K-bentonite

The data for K-bentonite given in table 9 are similar to those for Na-bentonite in that they indicate a distorted Hencricks-Jefferson structure to be present on the clay at low coverage. However, in the case of K-clay, the better fit of the exchangeable cations into the

---

[17] Calculated by subtracting twice the hydrogen bond energy of liquid water at 25° C. (4.6 kcal. per mole, 48, p. 214) from the heat of vaporization (10.5 kcal. per mole) at the same temperature.

hexagonal cavities of the mineral surface would seem to promote a longer duration of the Hendricks-Jefferson structure than on Na-clay; the data for K-bentonite at 0.4 monolayer water content enforce this supposition, although a strongly absorbing (cf. figure 7), 2.89 A. bond has made its appearance, indicating that some interference from the exchangeable cations has begun to occur.

As with the Na-clay, the water molecules on K-clay at low coverage appear to be in a transitory state at least until the monolayer has formed. Again, this is borne out by the fact that BET theory fails to describe water desorption on K-bentonite (41) until monolayer coverage occurs (as estimated from the adsorption data of Orchiston (43)). If the entropy of desorption is calculated as described previously and plotted against monolayer coverage, a decrease in the entropy of desorption between 0.2 and 0.3 coverage is observed, followed by a gradual increase until the monolayer has formed. The minimum probably reflects the entry of the exchangeable cations into the adsorbed water layer.

The mean hydrogen bond energy for the first monolayer on K-montmorillonite, calculated from the E_1 value given by Orchiston (43), is 5.0 kcal. per mole, in poor agreement with the 2.2 kcal. per mole found for the strongest absorbing hydrogen bonds (cf. figure 7) on K-clay, which should primarily limit desorption. The reason for the discrepancy probably lies in the fact that Orchiston's value comes from adsorption data rather than desorption data and that the structure of water on K-clay

at the monolayer water content is likely to be substantially different from that at lower coverage. However, more experimental information is required before a final decision can be made.

Water Adsorbed on Li-bentonite

Rowland, Weiss, and Bradley (50) found that the x-ray diffraction pattern for Li-bentonite behaved the same way during dehydration as did vermiculite. From this evidence they concluded that the structure of adsorbed water on the bentonite was the same as that determined by Mathieson and Walker (37, 38, 58) from a Fourier analysis of the diffraction pattern of Mg-vermiculite. The latter, it will be remembered, discovered that the exchangeable cations on the fully hydrated vermiculite are in octahedral coordination with two layers of adsorbed water molecules, resulting in average hydrogen bond lengths between the molecules as follows: H_2O-H_2O within a water layer near an exchange site, 2.97 A.; H_2O-H_2O between layers, 2.78 A.; and H_2O-O, 2.87 A. A bond 3.06 A. in length was postulated to occur between the octahedra surrounding the cations.

The data listed in table 10 support the conclusions of Rowland et al. (50).[18] Before the completion of the stable hydrate one would

---

[18] A two-layer structure is also implied for the water on Li-bentonite by the doublet observed near 3700 $cm.^{-1}$ in the spectrum of the hydrated clay (figure 6), each band center referring to nonhydrogen bonded OH groups in different water layers.

Table 10. Hydrogen Bond Lengths and Dissociation Energies in the Water Adsorbed by Li-and Ca-bentonite.

0.88 Monolayer Coverage[a]		1.00 Monolayer Coverage[a]	
Bond Length A.	Bond Energy kcal./mole	Bond Length[b] A.	Bond Energy kcal./mole
		Li-bentonite	
3.06	0.3	3.03	0.3
3.03	0.3	2.98	0.8
2.95	1.3	2.88	2.4
2.85	2.2	2.76	5.5
		2.71	7.6
1.2 Monolayers Coverage[a]		1.8 Monolayers Coverage[a]	
Bond Length[b] A.	Bond Energy kcal./mole	Bond Length A.	Bond Energy kcal./mole
		Ca-bentonite	
3.03	0.3	3.03	0.3
2.97	1.0	3.01	0.6
2.93	1.6	2.95	1.3
2.89	2.2	2.89	2.2
2.76	5.5	2.80	4.0
2.70	8.1	2.74	6.3

[a] Estimated from table 1 and the BET data of Mooney et al. (41).

[b] The higher unbonded OH stretching frequency (figures 6 and 7) was used in calculating these data; this arbitrary choice does not affect the results.

expect to find principally intralayer hydrogen bonds and H_2O-O bonds making up a monolayer; the bond lengths calculated for water on the dry clay film indicate that this is the case. On the hydrated clay film, hydrogen bond lengths of 3.03, 2.98, 2.88, 2.76, and 2.71 A. were observed, demonstrating that a distorted two-layer structure had begun to form despite the apparently low surface coverage.

One may regard the significant difference in structure between the water on Na- and K-bentonite and that on Li-bentonite as a manifestation of the electrostatic fields about the exchangeable cations on these clays. The effects of the fields on the water surrounding the cations is evident from the hydration numbers they have in dilute aqueous solution: 1.9 for K^+, 3.5 for Na^+, 7.1 for Li^+, and, for comparison, 12.0 for Ca^{+2} (21, p. 525). In accordance with this series, the exchangeable Li ions (and Ca ions, too, as will be shown presently) seem to have no difficulty superceding the clay surface at low water contents in influencing the adsorbed water structure; with exchangeable Na and K, as has been noted, this is not the case.

Water Adsorbed on Ca-bentonite

The x-ray diffraction pattern determined for Ca-bentonite by Rowland et al. (50) indicated that this clay likewise should have an associated water structure the same as that of Mg-vermiculite; this is also shown by the data in table 10. As with the water on Li-bentonite

and as Mathieson and Walker (38) suggested for that on Mg-vermiculite, the water structure on Ca-bentonite appears to be slightly distorted, the result of cationic diffusion and surface roughness.

From the E_1 value given by Orchiston (43) a mean hydrogen bond energy of 5.6 kcal. per mole can be estimated for the first BET "monolayer" on Ca-montmorillonite. Assuming, reasonably, that vaporization is limited by the strongest absorbing hydrogen bonds in the infrared spectrum, the calculated value of 2.2 kcal. per mole should be compared with that derived from adsorption data. The agreement between the two figures is poor, probably because Orchiston's E_1 value includes a sizeable contribution from the heat of dehydration of the exchangeable cations.

It is perhaps more than a coincidence that the bond energy of 6.3 kcal. per mole, the strongest in the water on hydrated Ca-bentonite, is in close agreement with the 6.0 kcal. per mole determined by Anderson et al. (2) as the apparent activation energy for the infiltration of water through a Ca-bentonite having the same initial moisture content as the hydrated Ca-clay film used in this study. The proximity of the data is further support for the hypothesis of Anderson et al. that the rupturing of the strongest hydrogen bonds among the preadsorbed water molecules is intimately involved in the rate-determining processes for unsaturated flow.

CONCLUSIONS

The experimental evidence reviewed and that derived from this investigation verify the general hypothesis proposed early in the thesis concerning the nature of adsorbed water. Water structures characterized as molecular associations subject to changes in organization whenever the adsorptive force field about them varies appear to be present on Li-, Na-, K-, and Ca-bentonite at relative humidities up to 15 per cent. This is more so for the Na- and K-clays, where the exchangeable cations can exert little more influence on the adsorbed water molecules than does the mineral surface, with the result that, until a monolayer is present, molecular orientation is sensitive to water content and an unmodified BET theory cannot account for the desorption isotherms of these clays. On the Li- and Ca-clays, although their exchangeable cations can and do wrest control of the water molecules from the clay surface forces and BET theory is obeyed, a water structure in a dynamic state is still present: The postulated distortion of the two-layer octahedra by cationic diffusion and surface faults implies a continual reorganization of molecular arrangement.

It should be remembered that these remarks apply to the state of water on bentonites undergoing a desorption cycle. Until the phenomenon of hysteresis has been satisfactorily explained any extension of them to the water on clays in an adsorption cycle is not wholly warranted. Moreover, although the conclusions given here represent, in the writer's opinion, as reasonably accurate a picture of adsorbed water as can be drawn at present, they must be regarded as in the nature of a hypothesis awaiting further experimental verification. In short, the quantitative solution to the problem of the structure of adsorbed water poses itself as the resultant of many factors participating in an, as yet, generally unknown mechanism. The resolution of this problem, contingent upon more experimental data on the micro-behavior of adsorbed water, will finally present itself in the form of a set of differential equations whose properties are amenable to describing the complex, continually altering interactions between water molecules and adsorptive force fields.

BIBLIOGRAPHY

1. Adler, H. H., Bray, E. E. et al. Infrared spectra of reference clay minerals. American Petroleum Institute Project 49, preliminary report 8, New York, 1950.

2. Anderson, D. M., Linville, A., and Sposito, G. Temperature fluctuations at a wetting front: III. Apparent Activation energies for water movement in the liquid and vapor phases. In Press.

3. Anderson, D. M.,and Low, P. F. The density of water adsorbed by lithium-, sodium-, and potassium-bentonite. Soil Sci. Soc. Amer. Proc. 22:99-103, 1958.

4. Barshad, I. The nature of lattice expansion and its relation to hydration in montmorillonite and vermiculite. Am. Mineralogist 34:675-84, 1949.

5. Bernal, J. D.,and Fowler, R. H. A theory of water and ionic solution, with particular reference to hydrogen and hydroxyl ions. J. Chem. Phys. 1:515-48, 1933.

6. Beutelspacher, H. Infrarot-untersuchungen an bodenkolloiden. Trans. Sixth Intern. Congr. Soil Sci., Reports B (Commission I). :329-35, 1956.

7. Bower, C. A., and Gschwend, F. B. Ethylene glycol retention by soils as a measure of surface area and interlayer swelling. Soil Sci. Soc. Amer. Proc. 16:342-45, 1952.

8. Brunauer, S., Emmett, P. H., and Teller, E. Adsorption of gases in multimolecular layers. J. Am.Chem. Soc. 60:309-19, 1938.

9. Buswell, A. M., and Dudenbostel, B. F. Spectroscopic studies of base exchange materials. J. Am. Chem. Soc. 63:2554-58, 1941.

10. Buswell, A. M., Krebs, K., and Rodebush, W. H. Infrared studies. III. Absorption bands of hydrogels between 2.5 and 3.5 μ. J. Am. Chem. Soc. 59:2603-5, 1937.

11. Callen, H. B.
Thermodynamics. John Wiley and Sons, Inc., New York, 1960.

12. Chako, N. O. Absorption of light in organic compounds. J. Chem. Phys. 2:644-53, 1934.

13. Cornet, I. Expansion of the montmorillonite lattice on hydration. J. Chem. Phys. 18:623, 1950.

14. Dwyer, R. J., and Oldenberg, O. The dissociation of H_2O into H + OH. J. Chem. Phys. 12:351-61, 1944.

15. Farmer, V. C. The infrared spectra of talc, saponite, and hectorite. Mineral. Mag. 31:829-45, 1958.

16. Forslind, E. Some remarks on the interaction between the exchangeable ions and the adsorbed water layers in montmorillonite. Trans. Fourth Intern. Congr. Soil Sci. 1:110-13, 1950.

17. Fox, J. J.,and Martin, A. E. Investigations of infrared spectra (2.5-7.5 μ). Absorption of water. Proc. Roy. Soc. (London) 174A: 234-62, 1940.

18. Fripiat, J. J., Chaussidon, J., and Touillaux, R. Study of dehydration of montmorillonite and vermiculite by infrared spectroscopy. J. Phys. Chem. 64:1234-41, 1960.

19. Giguere, P. A., and Harvey, K. B. On the infrared absorption of water and heavy water in condensed states. Can. J. Chem. 34: 798-808, 1956.

20. Greinacher, E., Luttke, W., and Mecke, R. Infrarot-spektroskopische Untersuchungen an Wassar, gelost in organischen Losungsmitteln. Z. Elektrochemie 59:23-30, 1955.

21. Harned, H. S. and Owen, B. B.
The Physical Chemistry of Electrolytic Solutions. Reinhold Publ. Co., Inc., New York, 1958.

22. Hendricks, S. B., and Jefferson, M. E. Structures of kaolin and talc-pyrophyllite hydrates and their bearing on water sorption of the clays. Am. Mineralogist 23:863-75, 1938.

23. Hendricks, S. B., Nelson, R. A., and Alexander, L. T. Hydration mechanism of the clay mineral montmorillonite saturated with various cations. J. Am. Chem. Soc. 62:1457-64, 1940.

24. Herzberg, G.
Infrared and Raman Spectra of Polyatomic Molecules. D. Van Nostrand Co., Inc., New York, 1945.

25. Hodgman, C. D., editor.
Handbook of Chemistry and Physics. Chemical Rubber Publ. Co., Cleveland, Ohio, 1960.

26. Jackson, M. L.
Soil Chemical Analysis. Prentice-Hall, Englewood Cliffs, New Jersey, 1958, pp. 459-62.

27. Kakitani, S. Infrared absorption by some clay minerals (OH-stretching vibration of montmorillonite, kaoline, and halloysite). Kobutsugaku Zasshi 3:49-52, 1956. (abs.)

28. Kerr, P. F., Hamilton, P. K. et al. Analytical data on reference clay minerals. American Petroleum Institute Project 49, preliminary report 7, New York, 1950.

29. Lippincott, E. R. Derivation of an internuclear potential function from a quantum-mechanical model. J. Chem. Phys. 26:1678-85, 1957.

30. Lippincott, E. R. and Schroeder, R. One-dimensional model of the hydrogen bond. J. Chem. Phys. 23:1099-1106, 1955.

31. Lonsdale, K. The structure of ice. Proc. Roy Soc. (London) 247A: 424-34, 1958.

32. Low, P. F. The apparent mobilities of exchangeable alkali metal cations in bentonite-water systems. Soil Sci. Soc. Amer. Proc. 22:395-8, 1958.

33. Low, P. F. Viscosity of Water in Clay Systems. Proc. 8th Natl. Conf. on Clays and Clay Minerals. Pergamon Press, New York. pp. 170-82, 1960.

34. Low, P. F. Physical Chemistry of clay-water interaction. Advances in Agron. 13:269-327, 1961.

35. Macey, H. H. Clay-water relationships and the internal mechanism of drying. Trans. British Ceram. Soc. 41:73-121, 1942. (abs.)

36. Mackenzie, R. C. Some notes on the hydration of montmorillonite. Clay minerals Bulletin I:115-19, 1950. (abs.)

37. Mathieson, A. McL. Mg-vermiculite: a refinement and re-examination of the crystal structure of the 14.36 A. phase. Am. Mineralogist 43:216-27, 1958.

38. Mathieson, A. McL., and Walker, G. F. Crystal structure of magnesium-vermiculite. Am. Mineralogist 39:231-55, 1954.

39. Mering, J. On the hydration of montmorillonite. Trans. Faraday Soc. 42B:205-19, 1946.

40. Mooney, R. W., Keenan, A. G., and Wood, L. A. Adsorption of water vapor by montmorillonite. I. Heat of desorption and application of BET theory. J. Am. Chem. Soc. 74:1367-71, 1952.

41. Mooney, R. W., Keenan, A. G., and Wood, L. A. Adsorption of water vapor by montmorillonite. II. Effect of exchangeable ions and lattice swelling as measured by x-ray diffraction. J. Am. Chem. Soc. 74:1371-74, 1952.

42. Ockman, N. The infrared and raman spectra of ice. Advances in Phys. 7:199-220, 1958.

43. Orchiston, H. D. Adsorption of water vapor: III. Homoionic montmorillonites at 25° C. Soil Sci. 79:71-78, 1955.

44. Ovcharenko, F. D., Neimark, I. E., Slinyakova, I. B., and Bykov, S. F. Heat of wetting of bentonite. Dopovidi Akad. Nauk. Ukr. R.S.R. 447-51, 1952. (abs.)

45. Pauling, L.
The Nature of the Chemical Bond. Cornell Univ. Press, Ithaca, New York, 1960.

46. Pauling, L., and Wilson, E. B.
Introduction to Quantum Mechanics. McGraw-Hill Book Co., New York, 1935.

47. Peterson, S. W., and Levy, H. A. A single-crystal neutron diffraction study of heavy ice. Acta Cryst. 10:70-76, 1957.

48. Pimentel, G. C., and McClellan, A. L.
The Hydrogen Bond. W. H. Freeman and Co., San Francisco, 1960.

49. Rojansky, V.
Introductory Quantum Mechanics. Prentice-Hall, Inc., New York, 1938.

50. Rowland, R. A., Weiss, E. J., and Bradley, W. F. Dehydration of monoionic montmorillonites. Clays and Clay Minerals. Nat. Acad. Sci.--Nat. Research Council Pub. 456:85-95, 1956.

51. Roy, D. M., and Roy, R. Hydrogen-deuterium exchange in clays and problems in the assignment of infrared frequencies in the hydroxyl region. Geochim. et Cosmochim. Acta 11:72-85, 1957.

52. Serratosa, J. M., and Bradley, W. F. Determination of the orientation of OH bond axes in layer silicates by infrared absorption. J. Phys. Chem. 62:1164-7, 1958.

53. Slabaugh, W. H. Heats of immersion of some clay systems in aqueous media. J. Phys. Chem. 59:1022-24, 1955.

54. Takizawa, M. Mechanism of water vapor adsorption on bentonite. J. Sci. Research Inst. (Japan) 54:313-22, 1960. (abs.)

55. Van Panthelon van Eck, C. L., Mendel, H., and Fahrenfort, J. A tentative interpretation of the results of recent x-ray and infrared studies of liquid water and H_2O-D_2O mixtures. Proc. Roy. Soc. (London) 247A:472-81, 1958.

56. Van Thiel, M., Becker, E. D., and Pimental, G. C. Infrared studies of hydrogen bonding of water by the matrix isolation technique. J. Chem. Phys. 27:486-90, 1957.

57. Walker, G. F. The mechanism of dehydration of Mg-vermiculite. Clays and Clay Minerals. Nat. Acad. Sci.--Nat. Research Council Pub. 456:101-15, 1956.

58. Walker, G. F. "Vermiculite Minerals," in The X-ray Identification and Crystal Structures of Clay Minerals. G. Brown, ed. Mineralogical Society, London, 1961, pp. 297-324.

59. Williamson, W. O. The clay-water relationship. Research 1: 363-68, 1948. (abs.)

60. Zemansky, M. W.
Heat and Thermodynamics. McGraw-Hill Book Co., Inc., New York, 1957.

61. Zettlemoyer, A. C., Young, G. J., and Chessick, J. J. Studies of the surface chemistry of silicate minerals. III. Heats of immersion of bentonite in water. J. Phys. Chem. 59:962-65, 1955.

LIST OF SYMBOLS

A.	angstroms
A, B, C, D	arbitrary constants appearing in the solution of the Schrödinger equation
ASTM	American Society for the Testing of Materials
a	width dimension of a crystal lattice
a	potential well center spacing; delta-function spacing
a_2b_1/a_1b_2	ratio of constants in the definition of E_1
B	constant in the definition of V_4
BET	Brunauer-Emmett-Teller
b	length dimension of a crystal lattice
b	constant in the definition of V_3
b_0, b_1, b_2	coefficients in the power series expansion of the delta-function spacing
C	BET constant
c	speed of light in vacuo
c	constant in the solution of the Schrödinger equation, $\psi(x)$
c	height dimension of a crystal lattice
c, c_1, c_2	constants in the internuclear potential function, V(r)
$c_v(T)$	heat capacity at constant volume as a function of temperature
D_e	dissociation energy of a hydrogen-like molecule
D_e, D_e^*	dissociation energies of the two bonds coalesced to make a hydrogen bond.
d_1	constant in the solution of the Schödinger equation, $\psi(x)$
E	total energy of a particle

$E(r)$	internuclear potential function
E_o	zero-point energy of an oscillator
E_1	heat of desorption of adsorbed water at monolayer coverage
E_1, E_2	total energies of the electrons in the double potential well
E_v	heat of vaporization of liquid water
e	base of the natural logarithms
e	charge of the electron
e.u.	entropy units: cal. per deg.
exp	exponential
g	"strength" of the delta-function
g	proportionality constant between n and n^*
H	Hamiltonian of a particle
h	Planck's constant
$\hbar$	Planck's constant divided by 2π
i	$\sqrt{-1}$
k	constant in the Schrödinger equation
k	Boltzmann's constant
k_e	equilibrium force constant of a chemical bond
k_H	hydroxyl stretching force constant
$k_{O \ldots O}$	hydrogen bond stretching force constant
L	Lagrangian of a particle
lim	limit
ln	natural logarithm
m	mass of a particle
m	exponent in the definition of V_4
n	constant in E(r)
n, n^*	constants in the hydrogen bond potential function
P	vapor pressure
P	legendre transform of L with respect to velocity
$\dot{p}$	first time derivative of the Legendre transform

p_x	momentum of a particle in one dimension
$(\delta Q/\delta m)_T$	slope of a heat of immersion--initial water content plot
q_{diff}	differential heat of desorption
q_{iso}	isosteric heat of desorption
R	ideal gas constant
R	hydrogen bond length
R_e	equilibrium hydrogen bond length
r	internuclear distance
r_e, r_e^*	equilibrium internuclear distances in the hydrogen bond potential function
T	absolute temperature
$T(\dot{x})$	kinetic energy of a particle as a function of speed
t	time
U_o	molar internal energy at absolute zero
u(T)	molar internal energy as a function of temperature
V(x)	potential function in one dimension
V(r)	internuclear potential function
V	hydrogen bond potential function
V_1, V_2	hydroxyl potential function
V_3	van der Waals repulsion energy
V_4	electrostatic potential function
V_e	$\lim_{R \to R_e} V_3 + V_4$
x	position coordinate
$\dot{x}$	first time derivative of x, speed
$\ddot{x}$	second time derivative of x, acceleration
x_o	width of a potential well
$\mathcal{A}$	operator to be associated with a dynamical variable, α
$[\alpha, \beta]$	Poisson bracket of α and β, $\partial(\alpha, \beta)/\partial(d, \beta)$

β	operator to be associated with a dynamical variable, β
Δr^2	$(r-r_e)^2$
$\delta(x)$	delta-function
$\delta(x-a)/2$	delta-function for the right hand side of a double potential well
$\delta(x+a)/2$	delta-function for the left hand side of a double potential well
θ	Debye temperature
λ	wave length
μ	micron
μ	reduced mass of a harmonic oscillator
ν	wave number
ν_2	bending vibration wave number
$2\nu_2$	combination of the bending vibration wave number
ν_3	unbonded OH stretching mode wave number
ν_3'	hydrogen-bonded OH stretching mode wave number
ν_T	translational mode wave number
π	3.1416
$\psi(x)$	solution of the Schrödinger equation
ψ''	second derivative with respect to x of $\psi(x)$
ψ^2	probability density for the particle described by $\psi(x)$
ω_o	zero-point frequency of vibration
ω_e	unbonded hydroxyl stretch frequency
ω_H	hydrogen-bonded hydroxyl stretch frequency